scientific reports

Check for updates

OPEN

A 2D inflammatory co-culture model for investigating synovial fibroblast and macrophage interactions in rheumatoid arthritis

Madhumithra Thangadurai[1], Swaminathan Sethuraman[1,2] & Anuradha Subramanian[1,2]✉

Rheumatoid arthritis (RA), a chronic autoimmune disease, marked by sustained inflammation and joint destruction, largely driven by pathological interactions between fibroblast-like synoviocytes (FLS) and macrophages. Current *in vitro* and *in vivo* models fall short in replicating the complex synovial microenvironment of RA, hindering translational research. In this study, we developed a simplified yet physiologically relevant 2D co-culture system that models both acute and chronic RA phases by modulating the ratio of healthy FLS to M1-polarized macrophages, simulating the intimal synovial layer. Direct exposure of FLS to inflammatory macrophages led to marked activation, with significant upregulation of pro-inflammatory cytokines—TNF-α (1.57-fold), IL-1β (6.30-fold), and IL-6 (4.94-fold)—and elevated expression of matrix metalloproteinases MMP2 (2.05-fold) and MMP9 (37.61-fold), key mediators of joint degradation. Using a transwell system, indirect exposure further induced FLS invasion, reflecting chronic inflammatory progression. Therapeutic validation using methotrexate (MTX) demonstrated its anti-invasive effect on activated FLS, supporting the model's utility in drug screening. This co-culture platform effectively captures RA-specific cellular responses and inflammatory dynamics, offering a scalable, high-throughput-compatible system for mechanistic studies and therapeutic evaluation.

Keywords Rheumatoid arthritis, Synovial fibroblasts, Macrophages, 2D co-culture model, Inflammatory cytokines, MMPs, Methotrexate, In vitro disease modeling

Rheumatoid arthritis (RA) is a chronic autoimmune disorder driven by both genetic and environmental factors, primarily characterized by joint inflammation, but also affecting multiple organs and tissues[1]. In a healthy joint, resident synovial cells such as macrophage (M0) and fibroblast-like synoviocytes (FLS) maintain tissue homeostasis and regulate immune responses[2,3]. However, in RA, the synovium becomes enriched with activated form of these resident cells[4,5]. In the early stages of RA (Fig. 1), this cellular balance is disrupted as resting macrophages (M0) polarize into pro-inflammatory M1 macrophages. These cells secrete key cytokines such as TNF-α, IL-1β and IL-6 *via* multiple inflammatory signalling pathways, including Notch, JAK/STAT, NF-κB, and MAPK. This creates a complex immune loop that subsequently activates synovial fibroblasts[6]. Once activated, FLS contribute significantly to inflammation by secreting pro-inflammatory cytokines, (TNF-α, IL-1β, and IL-6) and acquiring migratory and invasion properties through the expression of cadherin-11, CD44, and matrix metalloproteases (MMPs)[7].

Several studies have reported that CD44 and cadherin-11 are markedly upregulated in RA synovial tissue compared to healthy joints, with expression levels correlating strongly with the degree of inflammation. This is especially evident in FLS, which are central to cell-adhesion and migration, and can further enhance CD44 expression, creating a feedback loop that sustains inflammation[8,9]. In chronic RA, a hypoxic synovial environment, promotes angiogenesis and facilitates the infiltration of neutrophils, T-cells, and B cells, ultimately leading to synovial hyperplasia[10]joint destruction and bone erosion[11]. M1 macrophages are considered early initiators of RA pathogenesis, while FLS are increasingly recognized as the key mediators of bone erosion and joint damage across multiple joints[12,13].

[1]Tissue Engineering & Additive Manufacturing (TEAM) Lab, Centre for Nanotechnology & Advanced Biomaterials, School of Chemical & Biotechnology, SASTRA Deemed University, Thanjavur, Tamil Nadu, India. [2]Anusandhan Kendra-1, Tissue Engineering & Additive Manufacturing (TEAM) Lab, Centre for Nanotechnology & Advanced Biomaterials (CeNTAB), School of Chemical & Biotechnology, ABCDE Innovation Centre, SASTRA Deemed University, Thanjavur 613 401, Tamil Nadu, India. ✉email: anuradha@bioengg.sastra.edu

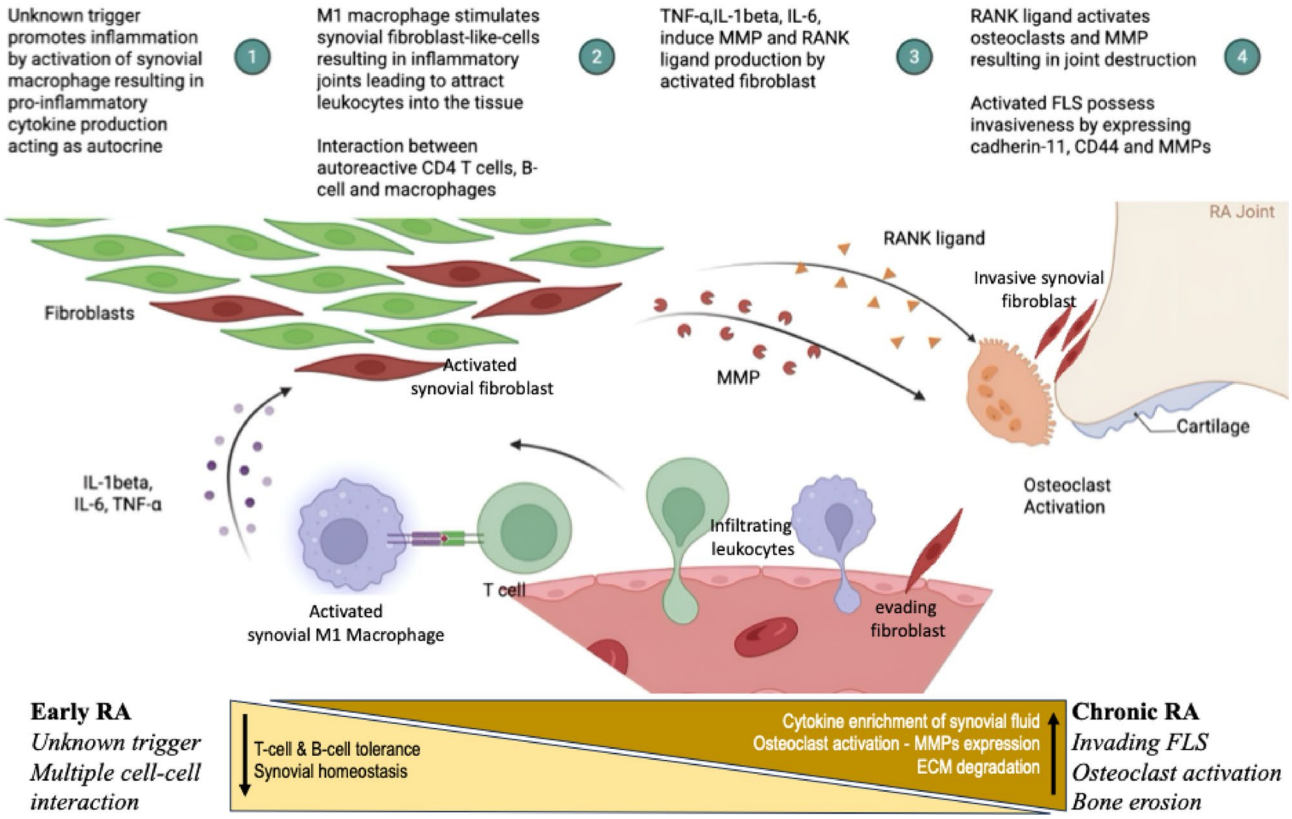

Fig. 1. Schematic representing sequential occurrence of pathophysiology from early to chronic RA.

However, current *in vitro* models, such as single–cell–type cultures, are limited in their ability to replicate the multi–cellular complexity and dynamic immune-synovial interactions, that are critical to RA pathogenesis. Although 3D culture systems and organoids offer a more tissue–like environment, they are often complex, time–consuming and poorly reproducible, limiting their suitability for high–throughput studies. Additionally, these models lack precise control over cellular composition and ratios, which is essential for studying RA progression from early to late stages[14]. Animal models such as collagen-induced arthritis (CIA), adjuvant-induced arthritis (AIA), and other experimental arthritis models recapitulate several features of RA, including immune cell infiltration, pannus formation, and cartilage destruction. However, these models are limited by significant species-specific differences, lack of genetic predisposition, and their inability to recapitulate the full spectrum of autoimmune features and heterogeneity characteristic of human RA[13–15]. Consequently, they offer limited insight into patient-specific disease mechanisms and therapeutic responses[16]. Despite the availability of disease-modifying antirheumatic drugs (DMARDs) such as Methotrexate, biologics targeting TNF-α, glucocorticoids like dexamethasone, many RA patients continue to exhibit suboptimal or highly variable responses to treatment[17]. This therapeutic inconsistency is largely attributed to the absence of physiologically relevant *in vitro* and *in vivo* models that can recapitulate the cellular complexity, immune dysregulation and patient-specific variability seen in human RA[18]. As a result, many drug candidates that show efficacy in preclinical models fail in clinical trials. This underscores the urgent need for advanced human-relevant RA models that accurately simulate disease mechanisms and predict therapeutic responses, thereby accelerating the discovery of novel therapeutic agents.

In this context, the present study employs a 2D co-culture system to investigate the crosstalk between macrophages and fibroblast-like synoviocytes. This model enables evaluation of macrophage-induced FLS activation, and highlights their role in promoting the invasive and migratory behaviors of synoviocytes—key features contributing to RA progression. This study focuses on activated FLS—either human synovial SW982 cells or primary synovial FLS isolated from rats—stimulated directly with cytokine-enriched conditioned media collected from M1 macrophages, which serves as an *in vitro* alternative to RA synovial fluid. These stimulated FLS were characterized for phenotypic changes and expression of pro-inflammatory cytokines, matrix metalloproteinases (MMPs), and CD44, a marker involved in cell-cell interaction and migration. Co-culture experiments involving primary rat FLS (rFLS) and THP-1 derived inflammatory M1 macrophages were conducted to validate the cross reactivity observed in the human SW982-M1 macrophage cell lines. The migration and invasion properties of FLS upon stimulation, which mimic those observed in chronic RA, were thoroughly investigated. Additionally, methotrexate (MTX) was employed as a model therapeutic agent to assess its efficacy in modulating activated FLS within the co-culture system, demonstrating the platform's utility for drug testing and molecular mechanistic studies.

Materials and methods

Cell lines such as THP–1 and SW982 cells and their respective media (Dulbecco's Modified Eagle Medium (DMEM) and Roswell Park Memorial Institute (RPMI–1640) medium were purchased from NCCS, Pune, and Hi–media, India, respectively. Fetal bovine serum (FBS) and phosphate–buffered saline (PBS) were purchased from Gibco, India. LPS (Lipopolysaccharide), Collagenase type II, 2',7'–dichlorodihydrofluorescein diacetate (H2DCFDA) were obtained from Sigma–Aldrich, USA. Lyso tracker Green DND-26, Invitrogen, USA. Corning® Transwell® polycarbonate membrane cell cultured inserts (pore size 0.8 µm) was purchased from Corning, USA. RNeasy mini kit (74104) was purchased from Qiagen, Germany. Primers and cDNA conversion were purchased from Eurofins, India. Protein concentrator (MWCO ~ 10 kDa) was purchased from Merck Millipore. RevertAid kit, and SYBR green master mix were purchased from Applied Biosystems, Thermo Fisher Scientific, USA. Primary antibodies such as Cadherin–11 (sc-365867), CD44 (NBP1-41266), Fibroblast specific protein (NBP1-89402), CD68 (ABM40050) and HIF–1α (3716 S) were purchased from Santa Cruz Biotechnology Inc., USA, Novus Biologicals, USA, Abbkine, USA and Cell signalling Technologies, USA, respectively.

Differentiation of THP–1 cells into inflammatory macrophages

The human monocyte cell line (THP–1) was maintained in RPMI 1640 cultured medium supplemented with 10% FBS and 1% penicillin–streptomycin. Cells were incubated at 37 °C in a humidified atmosphere containing 5% CO_2. To differentiate THP–1 monocytes into resting macrophages (M0), cells were treated with 100 nM phorbol 12–myristate 13–acetate (PMA) in RPMI–1640 media for 24 h. After incubation, the PMA-containing medium was aspirated and replaced with fresh RPMI-1640 medium. To further polarize the resting macrophage (M0) into a pro-inflammatory (M1) phenotype, 100 ng/mL of LPS was added and the cells were incubated for an additional 48 h. Following this stimulation period, the LPS-containing medium was removed and fresh LPS-free medium was added after thorough rinsing with PBS. The macrophages were then maintained for an additional 7 days, during which the culture medium was replaced with every alternate day with fresh LPS-free medium. The collected media, enriched with secreted pro-inflammatory cytokines, were pooled and concentrated using a protein concentrator. This cytokine-enriched conditioned medium was aliquoted and stored at − 80 °C for subsequent stimulation of fibroblast-like synovial cells. THP–1 monocytes, as well as the derived M0 and M1 macrophage populations, were fixed in 4% paraformaldehyde for further characterization.

Isolation of primary synovial fibroblast-like cells from rat

Male Wistar rats ($n = 12$), aged 6–8 weeks, and weighing 180–200 g were used for the isolation of primary synovial fibroblast-like cells, following approval from the Institutional Animal Ethics Committee (IAEC Approval number: 666/SASTRA/IAEC/RPP). All experimental procedures were conducted in accordance with the ARRIVE guidelines[19]. As illustrated in Fig. 2, the animals were euthanized using CO_2 inhalation, and both hind limbs were harvested and immersed in sterile 1X Hank's Balanced Salt Solution (HBSS). Under sterile

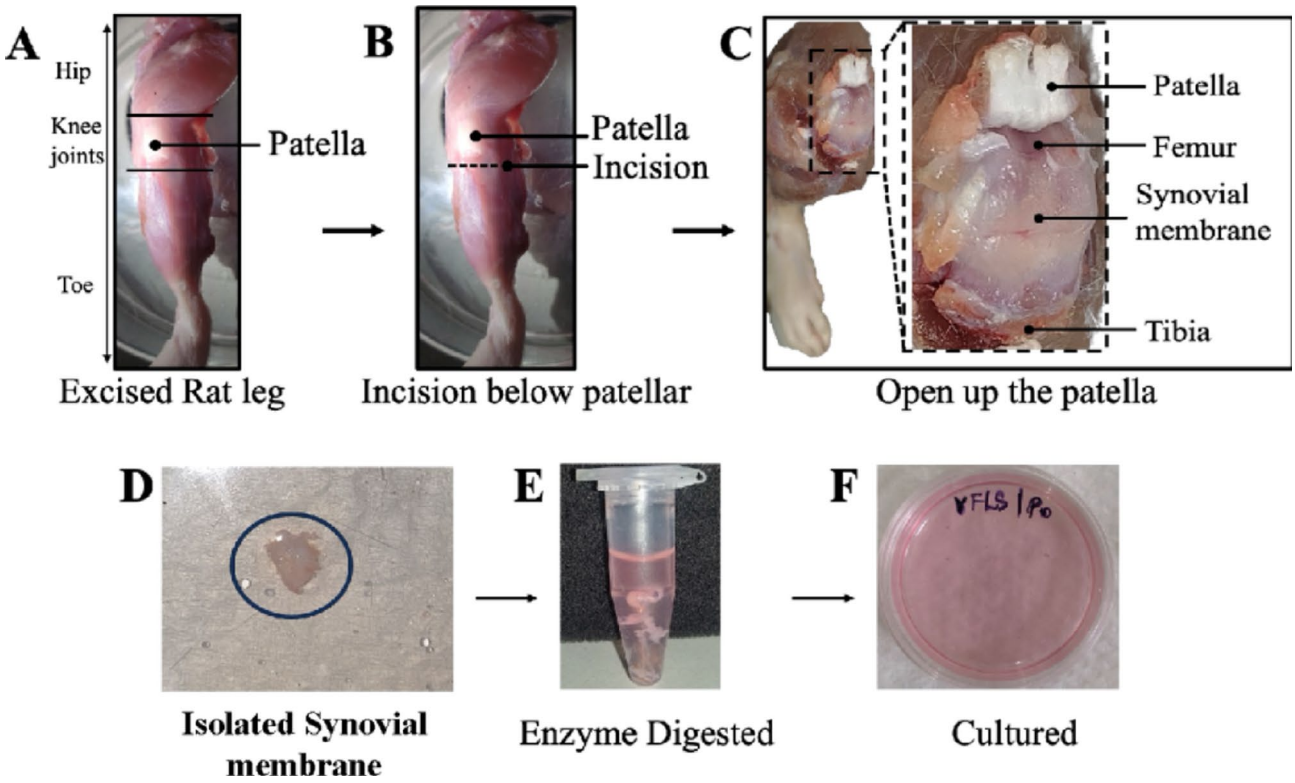

Fig. 2. Representative images of isolating fibroblast-like cells from rat synovium.

conditions, the excised limbs were surface sterilized using 10% Povidone–iodine solution for two minutes, followed by washing with 1X PBS. An incision was made below the patella to access the synovial membrane around the knee joint and the synovial tissue was isolated and chopped into pieces using butterfly scissors (Koshla Surgicals, Mumbai). The tissues were treated with DMEM media containing 2% collagenase II solution for 2 h, followed by the addition of FBS-containing media to neutralize the enzyme. The digested suspension was centrifuged at 3000 RPM for 10 min. The resulting cell pellet was resuspended in FBS–containing media and cultured in sterile TCPS plates. Cultures were maintained at 37 °C in a humidified atmosphere with 5% CO_2. Cells were passaged and primary synovial FLS were characterized after the fourth passage.

Development of inflammatory synovial fibroblast-like cells

The human synovial sarcomere cell line (SW982) and primary fibroblast–like synoviocytes (rFLS) from rat were cultured in DMEM medium supplemented with 5% FBS and 1% penicillin-streptomycin, and maintained at 37 °C in a humidified atmosphere containing 5% CO_2. At approximately 60% confluency, SW982 or rFLS cells were treated with 500 µL of concentrated inflammatory cytokine-enriched conditioned media for 48 h to induce their transformation into an inflammatory phenotype. Immediately following stimulation, morphological changes were monitored using a time–lapse video captured with the CytoSMART Lux live imaging system (Axion Biosystems). In addition, both inflammatory SW982 cell lines and rFLS primary cells were fixed and characterized for morphological and marker expression analysis (Fibroblast Specific Protein, cadherin–11 and CD44) using SEM and confocal laser scanning microscopy (CLSM) respectively. Further, gene expression analysis of pro-inflammatory cytokines (TNF–α, IL–1β and IL–6) for rFLS cells and (TNF–α, and IL–1β) for SW982 cells, cell adhesion and migration markers (Cadherin–11 and CD44), and matrix metalloproteases (MMP2, MMP3, MMP7, and MMP9) was performed using quantitative real-time PCR (qRT–PCR).

Cell migration

Cell migration following stimulation was assessed in activated SW982 cells and rFLS primary cells using a wound healing assay. Briefly, 2.5×10^4 cells were seeded into 6–well plates and cultured until they reached approximately 80% confluency. Stimulation was performed as described in earlier section . A scratch was introduced at the center of each well using a sterile pipette tip and optical images were captured at 0 and 48 h. The percentage of wound closure was calculated using the formula mentioned below. Non–stimulated cells were used as a control for the study.

$$Wound\ Closure\ (\%) = \frac{Area_{t=0} - Area_{t=\Delta t}}{Area_{t=0}} \times 100$$

Cell invasion assay

The effect of stimulation on cell invasion was evaluated in activated SW982 cell and rFLS cells using the Corning Transwell® assay. The bottoms of the inserts were coated with ECM–mimetic Matrigel® and incubated at 37 °C for 30 min. Subsequently, 1×10^4 fibroblast cells (SW982 or rFLS) were pre-stained using LysoTracker Green for 30 min, followed by washing with sterile PBS to remove any unbound dye. The green-labelled FLS were then seeded into the inserts containing FBS–free DMEM, while the lower well plates were filled with fresh serum-containing DMEM supplemented with cytokine-enriched conditioned media, including inflammatory cytokines. After 24 h of incubation, CLSM was performed to visualize the cells that had invaded through the Matrigel®, both before and after removing non-invaded cells from the insert. As a control, cells were cultured under identical conditions with only serum-containing DMEM in the lower wells, without inflammatory stimulation.

Development of an *in vitro* RA co-culture model

An *in vitro* rheumatoid arthritis model was established through co–culture of synovial fibroblast–like-cells (SW982 and rFLS cells) with macrophages (either M0 or M1 phenotype) at varying ratios – 2:1, 1:1 and 1:2. The macrophage cell density was adjusted to match a fixed FLS cell count of 2.5×10^4 cells/mL. These co-cultures were maintained for 72 h at 37 °C in a humidified atmosphere containing 5% CO_2.

Detection of ROS in co-cultured cells

To assess reactive oxygen species (ROS) production, the co-cultured cells (FLS: M0/M1 macrophages) 2:1, 1:1, and 1:2 ratios were incubated for 3 h with 2',7'–dichlorodihydrofluorescein diacetate (H2DCFDA) at a final concentration of 10 µM in serum-free DMEM, where a non-fluorescent compound that, upon oxidation by ROS, converts into a green fluorescent product. CLSM images were captured post-incubation to visualize ROS activity[20].

Cell–cell interaction in co-culture system

To evaluate the cross-reactivity between non-stimulated FLS and inflammatory macrophages (M1), co-culture experiments were conducted at a 1:2 ratio (FLS: M1). A time–lapse video was recorded using the CytoSMART Lux live imaging system (Axion Biosystems) to monitor cell–cell interactions and morphological changes. Co-cultures of non-stimulated rFLS with non-inflammatory macrophages (M0) served as control. Briefly, M0/ M1 macrophages were developed as described earlier. After differentiation, the cells were trypsinized and incubated with red fluorescent cell tracker dye for 30 min at 37 °C in a humidified 5% CO_2 atmosphere. Following two washes with PBS to remove excess dye, the pre-labelled M0/ M1 macrophages were seeded onto the adherent, non-stimulated FLS monolayer. After 2 h incubation period, real-time cellular interactions and morphological changes were recorded *via* time-lapse video using the CytoSMART Lux live imaging platform (Axion Biosystems). The co-culture of non-activated rFLS with M0 macrophages was used as the experimental control.

Cell invasion assay in co-culture system

The effect of stimulation on cell invasion was assessed in SW982 and rFLS cells using an indirect co–cultured RA model *via* the Corning Transwell® assay. The bottoms of the inserts were coated with ECM–mimetic Matrigel® and incubated at 37 °C for 30 min. Subsequently, green labelled fibroblast cells (1×10^4 SW982 or rFLS) suspended in FBS–free DMEM were seeded into the inserts. The lower wells were filled with fresh DMEM containing FBS and macrophage were seeded into the well plates to secrete inflammatory cytokines. After 24 h, confocal laser scanning microscopy images were acquired to visualize the fibroblast cells that had invaded through the Matrigel®, both before and after the removal of non-invaded cells from the inserts. This enabled the precise identification of fibroblast cells that had successfully migrated through the Matrigel®. Inserts cultured with FLS and wells plate containing only DMEM + FBS (without macrophages) served as control.

Drug testing in co-culture system

The effect of methotrexate (MTX) on the invasive properties of activated FLS, both SW982 and rFLS toward inflammatory macrophages was evaluated using the Transwell® assay set-up described previously. Briefly, 2 µg/mL of methotrexate was added to the inserts containing FLS and incubated at 37 °C, in 5% CO_2. After 24 h, the impact of MTX on cell invasion was assessed using confocal laser scanning microscopy images were captured before and after the removal of non-invaded cells from the inserts to visualize and quantify the number of FLS that had invaded the Matrigel® layer.

Scanning electron microscope

The morphological changes in synovial fibroblast-like cells and macrophages, before and after stimulation were determined using a scanning electron microscope (VEGA 3, Tescan). Briefly, the cells were fixed with 4% paraformaldehyde for 20 min, followed by a graded alcohol dehydration process. After complete drying, the sample coverslips were mounted onto carbon tape and gold-coated for 30 s using a sputter coater (JEOL, Japan). Images were acquired at an accelerating voltage of 10 kV.

Immunocytochemistry

The expression of cell-specific markers were analyzed by immunocytochemical staining using a Confocal Laser Scanning Microscope as reported elsewhere[21,22]. Briefly, cells were fixed with 4% paraformaldehyde for 30 min at room temperature and rinsed twice with PBS. The fixed cells were then permeabilized using citrate buffer for 20 min followed by blocking with a blocking solution containing 1% BSA and 0.1% Triton–X for 30 min. Subsequently, the cells were incubated with specific primary antibodies (1:500 or 1: 1000 dilutions) at 4 °C overnight, followed by incubation with secondary antibodies at room temperature for 3 h. Cell nuclei were counterstained using DAPI. Images were acquired at wavelengths of 405 nm (blue), 488 nm (green) and 594 nm (red) and the fluorescence intensities were quantified using Image J software.

Gene expression analysis

Total RNA was isolated from both non–stimulated and stimulated cells, including SW982 cells, rFLS, and M0/M1 macrophages, using a Qiagen Kit following the manufacturer's protocol. Briefly, cells were lysed with Trizol reagent for 10 min, followed by centrifugation at 12,000 RPM for 15 min at 4 °C. The supernatant was transferred to a fresh tube, mixed with 600 µL of 70% ethanol and incubated at 4 °C for 15 s. Subsequently, 700 µL of the mixer was transferred to a spin column and centrifuged at 10,000 RPM for 15 s. After the washing steps, purified RNA was eluted with 30 µL of RNase–free water. cDNA synthesis was performed using the Revertaid kit and the samples ($n = 3$) were used to determine gene expression levels as listed in supplementary Table 1 via qRT–PCR analysis (Applied Biosystems, Thermo Fisher Scientific). GAPDH was used as the internal control due to its relatively stable expression across various experimental conditions. Gene expression was quantified using the $2^{-\Delta\Delta CT}$ method and results were expressed as fold change normalized to the control.

Enzyme-linked immuno sorbent assay

Pro–inflammatory cytokines such as TNF–α, and IL–1β secreted by non–stimulated THP–1 cell, M0 macrophages, M1 polarized macrophages and SW982 cells were quantified using ELISA following the manufacturer's protocol. In addition, the secretion of TNF–α, IL–1β and IL–6 by non–stimulated and cytokine-stimulated primary rat synovial fibroblast–like synoviocytes (rFLS) was also assessed. To eliminate residual LPS, fresh culture media were added to the macrophage lineages following the initial48-hour stimulation, and conditioned media were subsequently collected. Similarly, rFLS were stimulated with cytokine-enriched conditioned media for 48 h, after which the media were removed to avoid confounding effects. The cells were then incubated in fresh DMEM for an additional 48 h and conditioned media were collected and stored at − 80 °C until analysis. Total protein content in the samples was determined using the BCA assay. For ELISA, samples ($n = 3$) were loaded into 96–well plates pre-coated with capture antibodies and incubated at 37 °C for 3 h. After washing with the provided buffer, specific detection antibodies were added and incubated for an additional 2 h at 37 °C. Following a final wash, the substrate solution was added, and absorbance was measured at the appropriate wavelength using a microplate reader. Cytokine concentrations were determined by comparing absorbance values to a standard calibration curve generated using GraphPad Prism.

Statistics

Statistical analyses were performed using Graph pad Prism 9.4 (Licensed). Data ($n = 3$) are expressed as mean ± standard error. Differences between group means were evaluated using Student's t–test, one–way ANOVA, or two-way ANOVA as appropriate. A p–value of < 0.05 was considered statistically significant.

Results and discussion

Polarization and characterization of inflammatory macrophages (M1) from THP-1 cells

THP–1 cell growing in suspension were differentiated into adherent resting macrophages (M0) after 24 h of PMA stimulation. Both THP-1 and M0 macrophages exhibited a round and smooth cell surface with an average diameter of 8.55 ± 0.21 mm^2 and 32.05 ± 1.48 µm respectively (**Supportive** Fig. 1B & C). The morphological characteristics of inflammatory macrophages (M1) became evident following LPS stimulation of resting (M0) macrophages for 48 h. Scanning electron micrographs (SEM) revealed that inflammatory macrophage (M1) displayed an amoeboid morphology with numerous spike–like cytoplasmic projections extending from their surface[23] and had a diameter of 50.70 ± 2.9 µm (**Supplementary Fig. 1D**). The differentiation into macrophages was further confirmed by the expression of the characteristic marker CD68 following LPS stimulation (**Supplementary Fig. 1F-I**). A significantly higher expression of CD44 was observed in the M1 macrophage lineage, aiding in cell-cell communication similar to that seen in native RA conditions. This further confirmed the inflammatory phenotype of M1 macrophages (Fig. 3A-D).

Gene and protein expression of macrophage lineage

Synovial macrophages contribute to the maintenance of tissue homeostasis, while infiltrating monocyte–derived inflammatory macrophages play a crucial role in upregulating pro–inflammatory cytokines. These cytokines, in turn, stimulate synovial cells to overexpress matrix metalloproteinases (MMPs), which contribute to bone erosion through the degradation of collagen and proteoglycans[24]. To assess the inflammatory profile, the gene expression of key cytokines was evaluated using qRT–PCR. Inflammatory macrophages (M1) exhibited significantly elevated expression levels of TNF–α (3.97 ± 0.16-fold) and IL–1β (149.18 ± 3.59-fold) compared to THP-1 cells and resting M0 macrophages (*$p < 0.05$) (Fig. 4A & B). Corresponding protein levels, measured by ELISA, also showed significantly increased expression of TNF–α (163.84 ± 12.58 pg/mL), IL–1β (85.72 ± 0.35 pg/mL) in M1 macrophages, aligning with qRT–PCR data (Fig. 4C & D). Further, qRT-PCR analysis of MMP gene expression revealed a significant upregulation of MMP2 (1.2 ± 0.17-fold), MMP3 (359.81 ± 27.98-fold) and MMP9 (127.93 ± 3.39-fold) in M1 macrophages compared to THP-1 and M0 macrophages (Fig. 4E–G). Additionally, a marked increase in the expression of CD44 (51.57 ± 2.49-fold), was observed in M1 macrophages (Fig. 4H), reinforcing its relevance as a key regulator of cell–cell, cell–matrix communications as well as cell migration – hallmarks of RA pathogenesis.

Development and characterization of stimulated rat fibroblast–like–Synoviocytes

Primary fibroblast–like–Synoviocytes (rFLS) was isolated from rat synovial tissue and stimulated for 48 h using concentrated cytokine-enriched conditioned media. The morphology and expression of RA specific biomarkers including fibroblast-specific protein (FSP), cadherin–11 (cad–11) and CD44 were analyzed before and after stimulation using scanning electron microscopy and laser confocal microscopy. SEM imaging revealed that the isolated rat FLS displayed a typical fibroblast morphology under resting conditions, whereas stimulation with cytokine-enriched conditioned media induced a pronounced elongated, spindle-shaped morphology (Fig. 5A & B). Live cell imaging demonstrated the dynamic phenotypic transformation of rFLS from a resting to an activated state upon exposure to the cytokine-rich media (Supplementary video 1 & 2). Immunofluorescence analysis confirmed the expression of fibroblast-specific markers - fibroblast specific protein (FSP) and cadherin–11 (cad–11) and CD44 in the isolated FLS, indicating their synovial fibroblast-like characteristics (Fig. 5C - E). Following 48 h of stimulation, there was notable upregulation in the expression levels of these markers (Fig. 5F - H). Notably, Cad–11 and CD44 are key mediators of cell migration and invasion, critical to the pathogenic role of activated fibroblast–like–cells in the RA synovium[25,26]. Quantitative morphological analysis revealed a significantly increased aspect ratio in stimulated rFLS cells (14.22 ± 0.88) compared to non–stimulated cells (2.44 ± 0.17), reflecting the morphological polarization associated with an activated state (Fig. 5I). Additionally, quantitative analysis of immunofluorescence-stained cells confirmed increased expression of FSP, cadherin–11 and CD44 following cytokine stimulation (Fig. 5J – L).

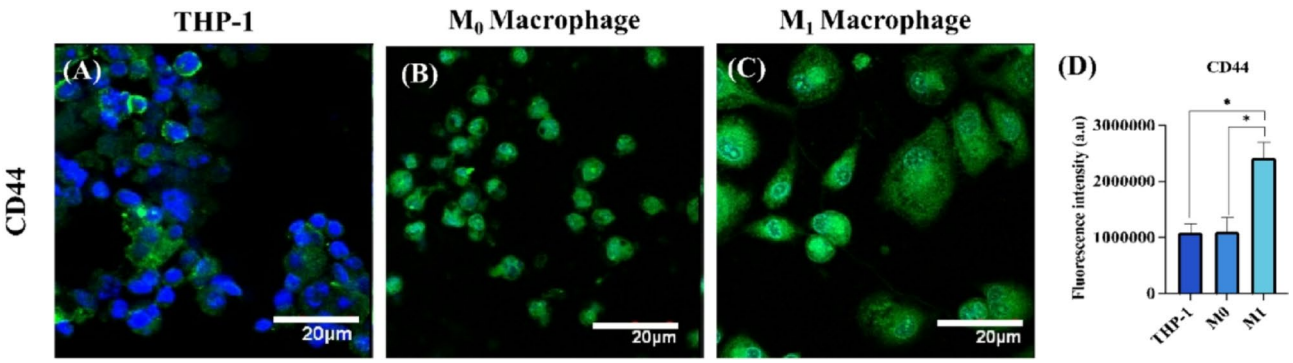

Fig. 3. (**A**–**C**) Representative CLSM images showing CD44 expression (green) in THP-1 cells, M0 macrophages, and M1 macrophages, nuclei were counter stained with DAPI (blue). Scale bar: 20 µm; (**D**) Quantitative analysis of CD44 expression in THP-1 cells, M0 macrophages and M1 macrophages using image J software (One way ANOVA, *$p < 0.05$).

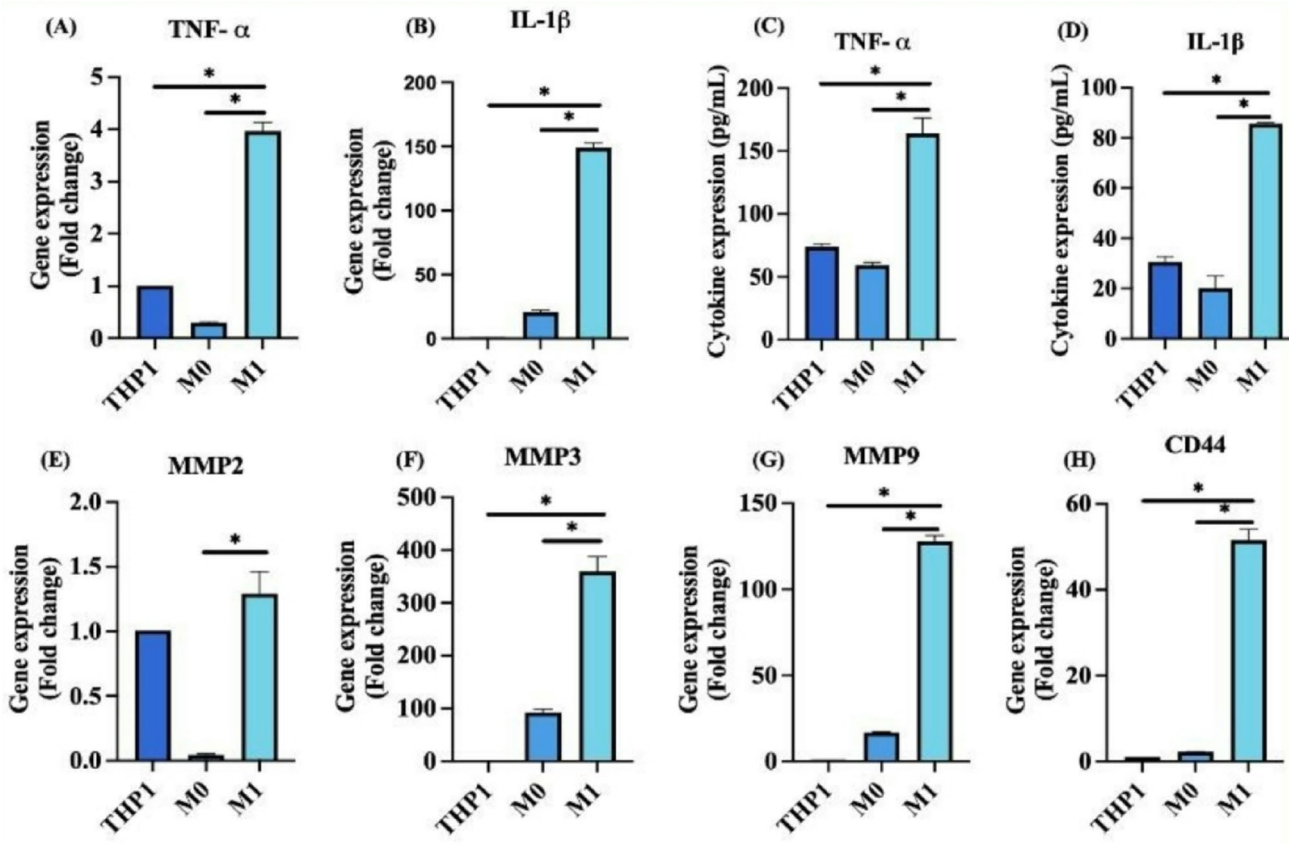

Fig. 4. (**A**, **B**) Gene expression levels of inflammatory cytokines TNF–α and IL–1β respectively, in THP-1, M0 and M1 macrophages, analyzed by qRT–PCR; (**C**, **D**) Quantification of TNF–α and IL–1β protein expression in resting and stimulated cells using ELISA; (**E**–**G**) Gene expression analysis of matrix metalloproteinase MMP2, MMP3, and MMP9 in THP-1, M0 and M1 macrophages; (**H**) Gene expression of CD44 in THP-1, M0 and M1 macrophage cells. ($n = 3$; One way ANOVA, $^*p < 0.05$).

Gene and protein expression of stimulated rat fibroblast–like– synoviocytes

The expression of marker genes such as Thy–1 (CD90) (1.37 ± 0.10-fold) and cadherin–11 (5.79 ± 0.30-fold), which are typically expressed by synovial fibroblast and are involved in maintaining synovial lining integrity, confirmed the fibroblast characteristic of the isolated rFLS from rat synovium (Fig. 6A & B). Upon stimulation with cytokine-enriched conditioned media for 48 h, the rFLS exhibited an upregulation in inflammatory cytokine gene expression including TNF–α (1.57 ± 0.007-fold), IL–1β (6.30 ± 0.17-fold) and IL–6 (4.94 ± 0.12-fold) compared to non–stimulated cells (Fig. 6C – E). ELISA quantification revealed significantly elevated secretion levels of these cytokines in stimulated FLS: TNF–α (558.29 ± 37.05 pg/mL), IL–1β (98.11 ± 0.66 pg/mL) and IL–6 (10096.64 ± 256.39 pg/mL) (Fig. 6F – H). The cytokines detected in the conditioned media (Fig. 6I) served as potent stimulants, triggering cytokine production in FLS. These secreted inflammatory mediators are known to induce CD44 and matrix metalloproteinase production[27]contributing to extracellular matrix remodeling and bone erosion. CD44 expression (1.79 ± 0.06-fold) was significantly increased, supporting enhanced cell–cell communication, cell–matrix interaction, migration and invasion. Additionally, the expression of MMP2 (2.05 ± 0.05-fold) and MMP9 (37.61 ± 0.89-fold) was significantly higher in stimulated FLS (Fig. 6J – L), consistent with their role in ECM-degradation and RA-associated joint destruction.

Migration and invasion potential of stimulated rFLS

As discussed earlier, the expression of various factors such as cadherin-11, CD44 and MMPs aids cellular migration and invasion. Therefore, the migratory and invasive characteristics of stimulated rFLS cells were evaluated. After 48 h of stimulation with cytokine-enriched conditioned media, rFLS demonstrated approximately 60% wound closure, indicating a significantly enhanced migration compared to non–stimulated control cells (Fig. 7A). Additionally, transwell invasion assays revealed that stimulated rFLS had greater invasive potential through ECM–mimetic Matrigel® toward a cytokine-enriched conditioned media with fresh media, compared to the non–stimulated group (Fig. 7C & D). This increased invasiveness is attributed to the cytokine-induced upregulation of MMP expression, mimicking inflammatory conditions observed in RA.

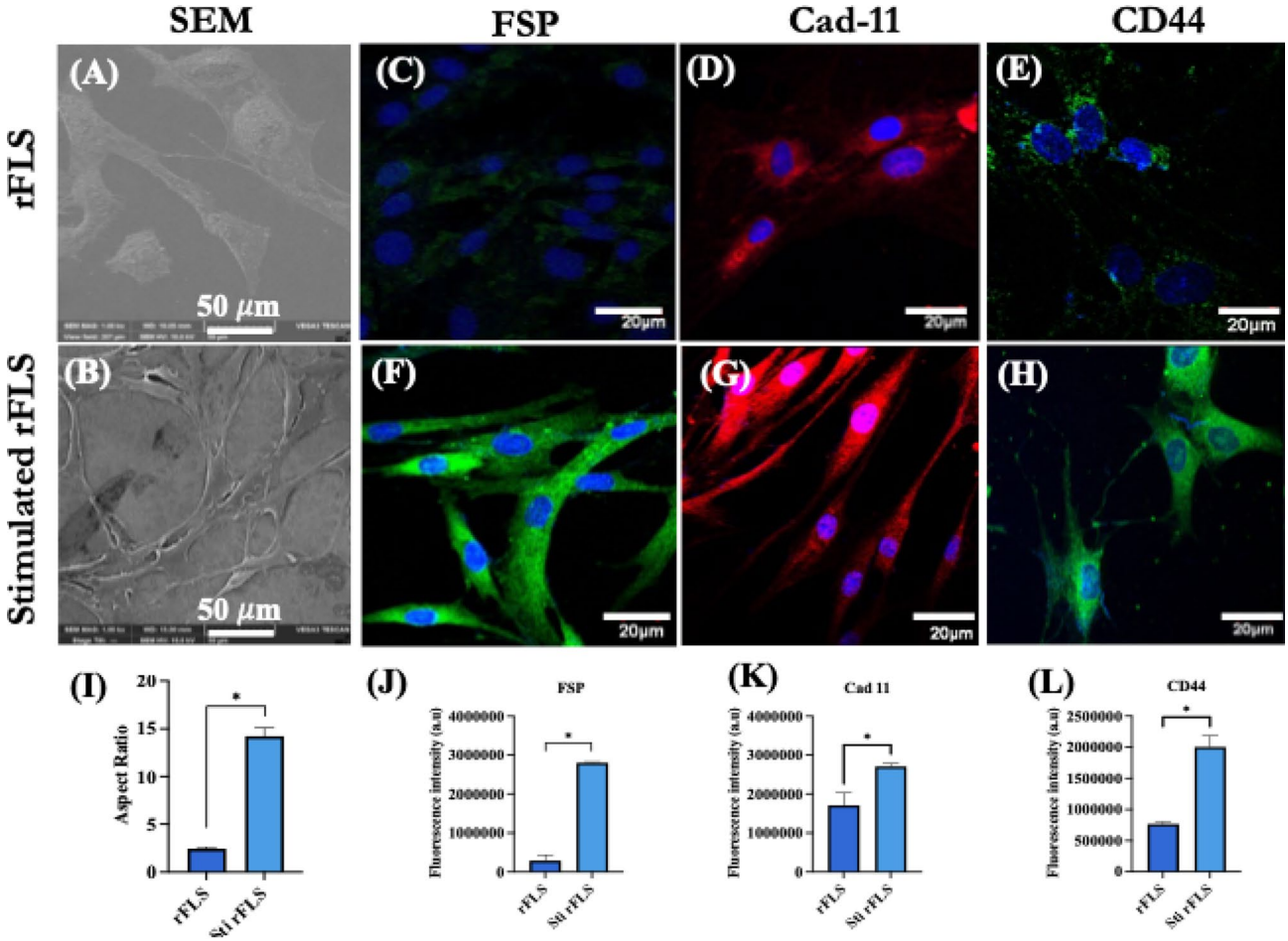

Fig. 5. (**A**, **B**) Representative SEM images of resting and stimulated synovial fibroblast-like cells from rat, respectively; (**C**–**E**) CLSM images of showing immunofluorescence staining of fibroblast specific protein (FSP), cadherin–11 (Cad–11) and CD44 of non–stimulated rFLS (Scale bar: 20 μm); (**F**–**H**) CLSM images of fibroblast specific protein (FSP), cadherin–11 (Cad–11) and CD44 of stimulated rFLS (Scale bar: 20 μm); (**I**) Quantification of the aspect ratio of non–stimulated and stimulated rFLS, indicating morphological polarization; (**J**–**L**) Quantitative fluorescence intensity analysis of fibroblast specific protein, cadherin-11 and CD44 in non–stimulated and stimulated rFLS (Student's t–test, $^{*}p < 0.05$).

Development and characterization of stimulated SW982 cells

Similarly, the human synovial sarcoma cell line SW982 was stimulated with inflammatory cytokine-enriched conditioned media for 48 h to mimic RA–FLS conditions[28,29]. Scanning electron microscopy revealed a spindle-shaped morphology in stimulated SW982 cells, with a significantly higher mean aspect ratio (3.95 ± 0.22) compared to non–stimulated cells (1.70 ± 0.04) (Fig. 8A, B & I). Both non–stimulated and stimulated SW982 cells were immunostained for fibroblast–specific protein (FSP), cadherin–11 (Cad–11) and CD44 key markers involved in cell migration, adhesion and tissue remodeling in RA synovium. Immunofluorescence images (Fig. 8C – E) confirmed that SW982 cells exhibited fibroblast-like synoviocytes (FLS) characteristics with significantly higher expression of these markers in the stimulated group (Fig. 8F – H). In RA pathology, CD44 drives cell migration and invasion by regulating MMPs activity and cytoskeletal dynamics[30,31]while cadherin–11 promotes tight cell clustering within inflamed and hyperplastic synovial tissue[26,32,33]. The elevated expression of FSP, CD44, and cadherin–11 in stimulated SW982 cells supports their use as an *in vitro* model resembling the hyperactive, migratory and invasive phenotype of RA-FLS (Fig. 8J – L).

Gene and protein expression of inflammatory SW982 cells

The inflammatory response of SW982 cells was further evaluated by assessing the gene and protein expression of key functional markers and inflammatory cytokines following stimulation with cytokine-enriched conditioned media. After 48 h of stimulation, the expression levels of pro–inflammatory cytokines (TNF–α and IL–1β), matrix-remodeling enzymes (MMPs: MMP2, MMP3, MMP7 and MMP9) and fibroblast–specific markers (Cadherin–11 and CD44) were evaluated. Quantitative PCR analysis revealed significant upregulation of cadherin–11 (7.08 ± 0.36-fold), CD44 (2.45 ± 0.14-fold) and pro-inflammatory cytokines such as TNF–α (1.726 ± 0.02-fold) and IL–1β (1.82 ± 0.16-fold) in stimulated SW982 cells compared to non–stimulated controls

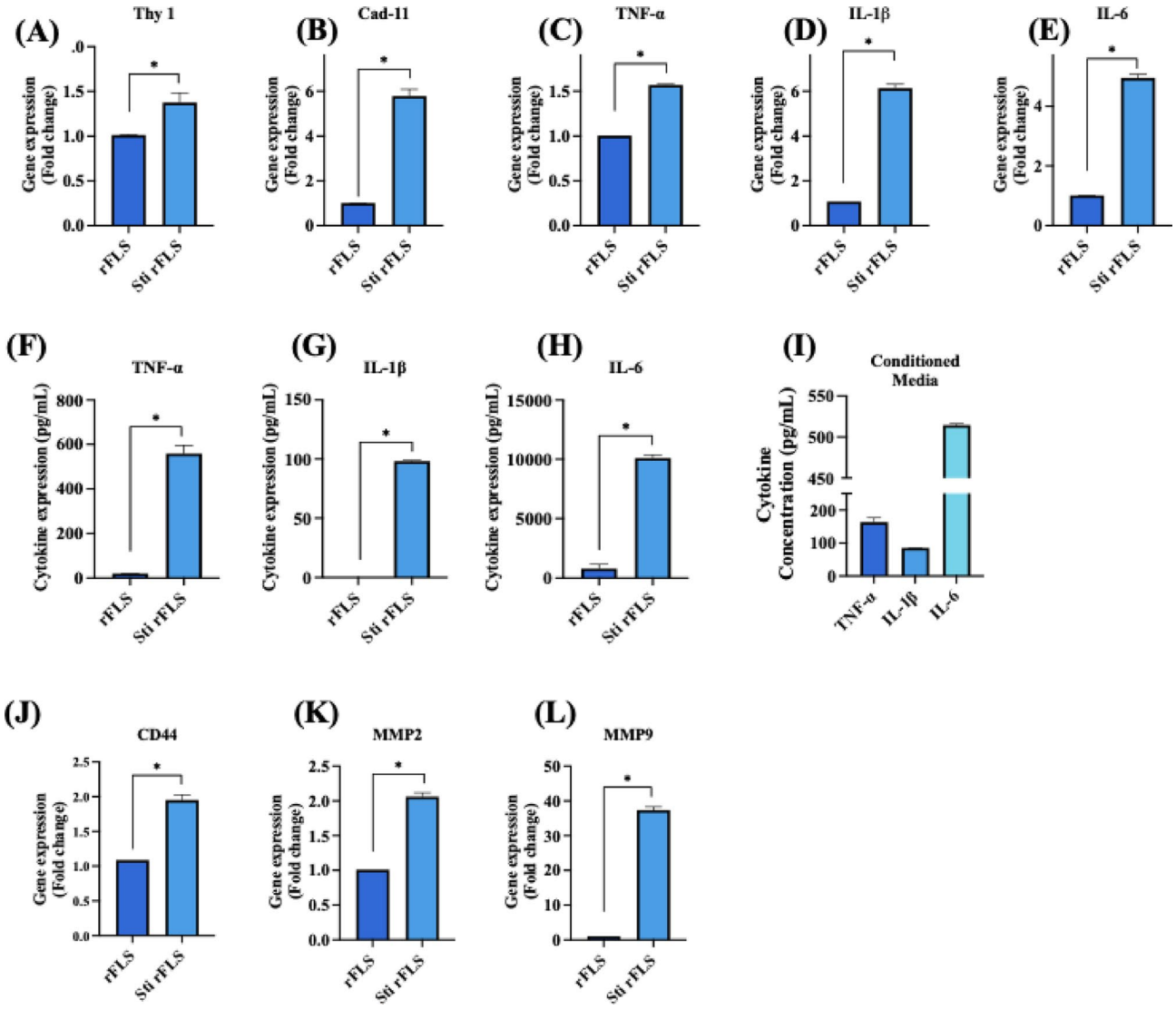

Fig. 6. Gene and protein expression profiles of non–stimulated and cytokine-stimulated rFLS cells. (**A**, **B**) Gene expression of synovial fibroblast markers Thy–1 and cadherin–11; (**C**–**E**) Gene expression of proinflammatory cytokines TNF–α, IL–1β and IL–6; (**F**–**H**) ELISA-based quantification of TNF–α, IL–1β and IL–6 secretion in non-stimulated vs. stimulated rFLS cells and (**I**) Cytokine concentrations in the macrophage-derived conditioned media used for FLS stimulation; (**J**–**L**) Gene expression of CD44, MMP2 and MMP9, in non-stimulated vs. stimulated rFLS cells ($n = 3$; Student's t–test, $^{*}p < 0.05$).

(Fig. 9A – D). These findings were corroborated by ELISA, which confirmed significantly elevated secretion of TNF–α (153.49 ± 6.04 pg/mL) and IL–1β (275.08 ± 32.15 pg/mL) by the stimulated cells ($p < 0.05$) (Fig. 9E & F). These results indicate that the cytokine-enriched conditioned media effectively induces a pro–inflammatory phenotype in SW982 cells, closely mimicking the cytokine expression profile of rheumatoid arthritis synovial fibroblasts. Further invasion potential of SW982 cells was evaluated through the expression of MMP2, MMP3, MMP7 and MMP9. qRT-PCR results showed a significant increase in MMP2 (1.86 ± 0.29-fold), MMP3 (1.85 ± 0.08-fold), MMP7 (12.62 ± 2.20-fold) and MMP9 (25.0 ± 0.30-fold) expressions in stimulated SW982 cells (Fig. 9G – J). These data confirm that cytokine stimulation successfully promotes an inflammatory phenotype characterized by enhanced matrix degradation activity. The significant upregulation of TNF–α and IL–1β indicates a robust pro–inflammatory response consistent with the cytokine milieu observed in RA joints. These cytokines are key mediators of synovial inflammation and fibroblast activation, contributing to joint destruction and synovial hyperplasia. Notably, elevated TNF–α levels are critical drivers of RA pathogenesis and are major therapeutic targets. Moreover, the upregulation of MMP2 and MMP9 expression highlights the enhanced invasive potential of stimulated SW982 cells. MMPs are crucial mediators of ECM degradation and are directly associated with cartilage and bone erosion in RA. Collectively, these findings suggest that cytokine-enriched conditioned media effectively mimics the inflammatory microenvironment of RA, driving both cytokine production and ECM-degrading enzyme expression in SW982 cells[34].

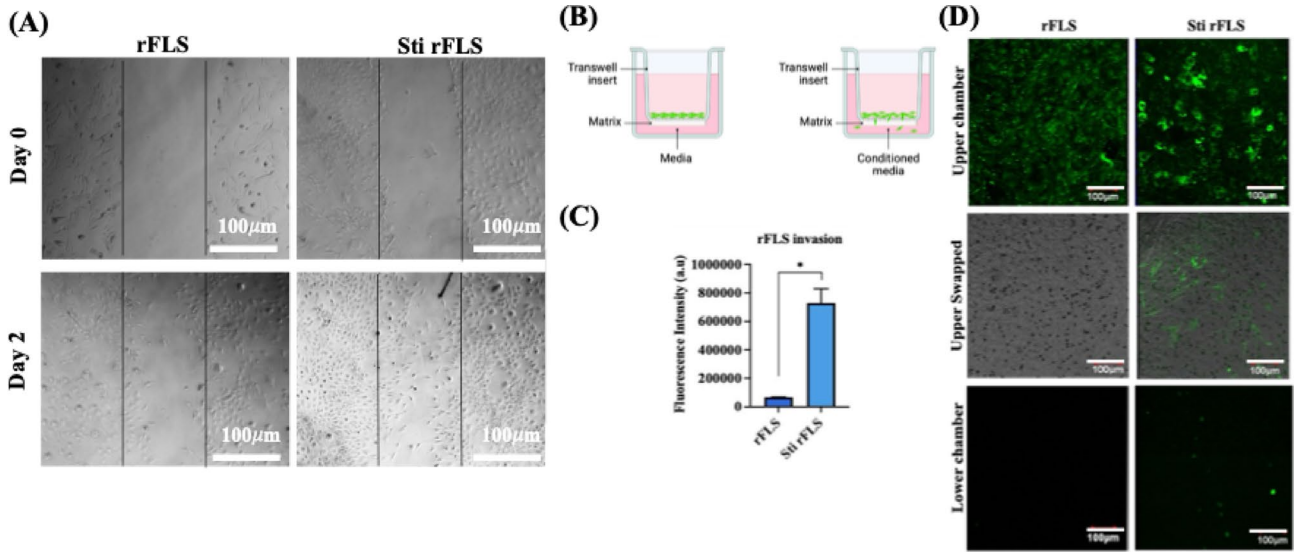

Fig. 7. (**A**) Time dependent wound closure analysis of non–stimulated and stimulated rFLS cells, (Scale bar: 100 μm); (**B**) Schematic representation of the transwell setup for the cell invasion assay; (**C**, **D**) Quantification of fluorescence intensity and representative CLSM images showing green-labelled rFLS invading through Matrigel® under cytokine-stimulated conditions (Scale bar: 100 μm). ($n = 3$; Student's t–test, $^*p < 0.05$).

Migration and invasion potential of stimulated SW982

The migratory and invasive behavior of stimulated SW982 cells following stimulation with cytokine-enriched conditioned media was evaluated using wound closure and Transwell invasion assays, as RA–FLS are known to contribute to ECM degradation and joint destruction through their aggressive migratory phenotype and invasive characteristics[35,36]. After 48 h of stimulation, SW982 cells demonstrated a marked closure, with approximately 80% of closure observed, compared to minimal closure in non–stimulated group (Fig. 10A). The Transwell assay setup is schematically represented in Fig. 10B. Invasion assays revealed that stimulated SW982 cells were capable of penetrating the ECM mimetic Matrigel® and migrating toward the chemoattractant present in the lower chamber. This was in sharp contrast to non–stimulated cells, which showed negligible invasion (Fig. 10C & D). The enhanced invasion of the stimulated SW982 cells is attributed to the cytokine-mediated upregulation of matrix metalloproteinases (MMPs), as demonstrated earlier by elevated MMP2, MMP3, MMP7, and MMP9 gene expression levels. The results highlight that cytokine-enriched conditioned media effectively induce an aggressive phenotype in SW982 cells, mimicking native RA-FLS behavior in promoting cartilage and bone damage through ECM degradation and tissue invasion.

Hypoxia-inducible factor 1α (HIF-1α) expression in activated synovial cells

Hypoxia-inducible factor 1 alpha (HIF-1α) exhibits distinct and pathologically relevant expression patterns within the synovial tissue of rheumatoid arthritis patients, playing a central role in disease progression and in sustaining the inflammatory microenvironment. Upon activation of M1 macrophages, SW982 and rFLS cells (Fig. 11A - D), HIF-1α expression demonstrated an increase in fluorescence intensity, consistent with the pro-inflammatory phenotype and its reliance on cytokine production[37]. In particular, the upregulation of HIF-1α in fibroblast-like synoviocytes (FLS), enhances the production of inflammatory cytokines and surface receptors involved in cell-cell interactions[38]. The chronic hypoxic conditions characteristic of RA joints contributes to sustained HIF-1α expression throughout the synovial membrane, thereby perpetuating the inflammatory response that defines RA pathophysiology[39]. The observations in stimulated rat fibroblast-like cells closely mirror those seen in the human SW982 cell line, further supporting the translational relevance of these findings. The upregulation of HIF-1α is indicative of hypoxic stress, which is known to drive synoviocytes proliferation and subsequent activation – key processes in RA progression[40].

Development of RA co-cultured *in vitro* model

In this study, an *in vitro* model of rheumatoid arthritis was established by co-culturing rat-derived fibroblast–like synoviocytes (rFLS) or SW982 cells with either M0 or M1 (pro-inflammatory) polarized macrophages. This model was designed to replicate the inflammatory microenvironment of RA joints, where macrophages are known to mediate the activation of resting synovial FLS. It serves as a valuable tool for investigating RA pathogenesis and evaluating potential therapeutic interventions. ROS levels were measured using DCFDA assays. The results demonstrated significantly elevated ROS production (Fig. 12A & B) in rFLS–M1 co–cultures (1:2 ratio) compared to rFLS–M0 co–cultures after 3 days ($p < 0.05$). This elevated ROS level suggests that M1 macrophages induce an oxidative stress environment, contributing to the pathological conditions observed.

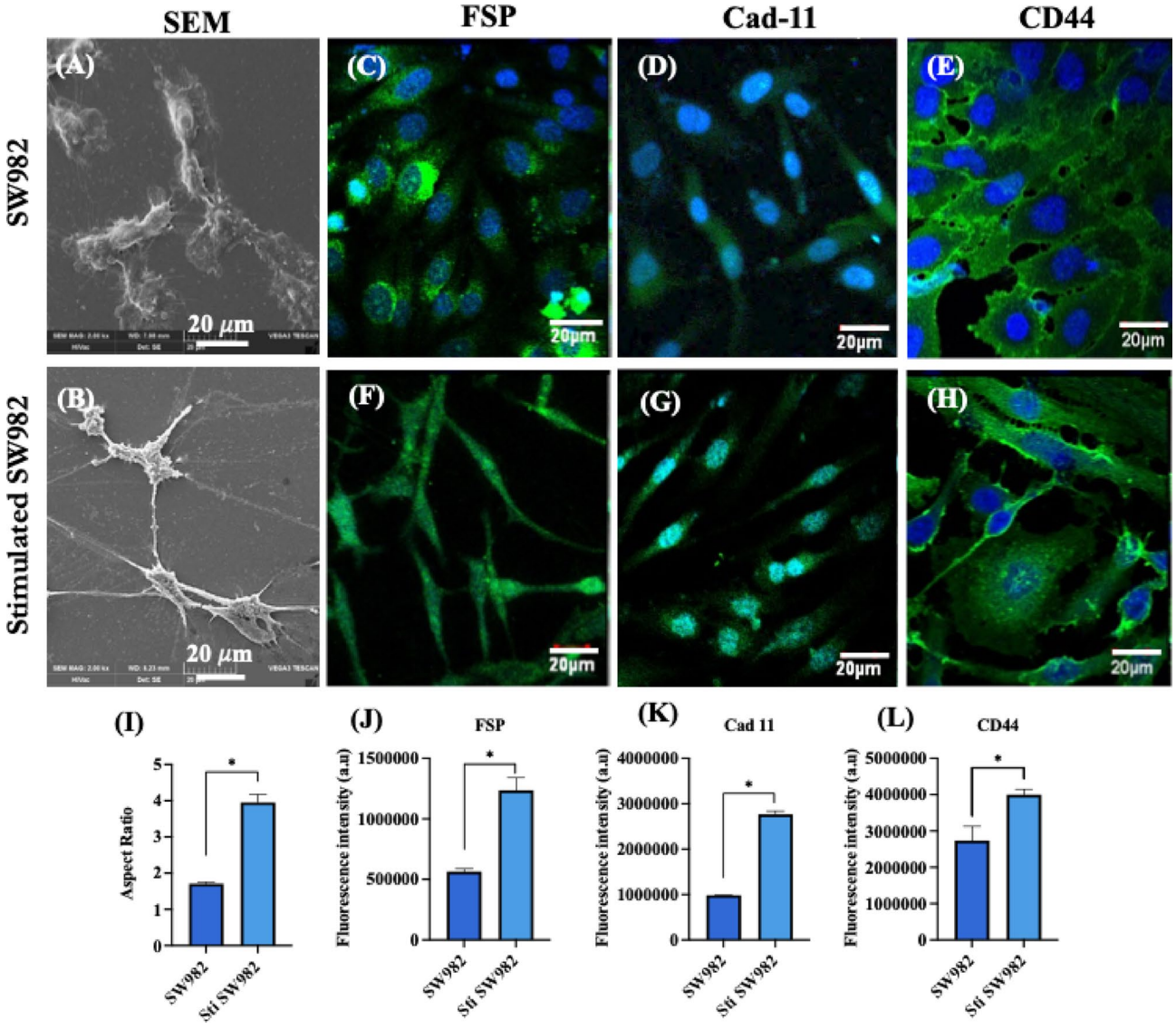

Fig. 8. (**A**, **B**) Representative SEM images of non-stimulated and stimulated SW982 cells; (**C**–**E**) Representative CLSM images showing immunofluorescence staining for fibroblast specific protein (FSP: green), cadherin–11 (Cad–11: green) and CD44 (green) in non-stimulated SW982 cells (**F**–**H**) Corresponding images for stimulated SW982 cells. All cells were counterstained with DAPI for nuclei visualization (blue) (Scale bar: 20 μm); (**I**) Quantification of the aspect ratio of non-stimulated and stimulated SW982 cells; (**J**–**L**) Quantitative fluorescence intensity analysis of FSP, Cad-11 and CD44 in non-stimulated and stimulated SW982 cells ($n = 3$; Student's t–test, $^*p < 0.05$).

Morphological changes in rFLS co-cultured with macrophages

Time–lapse imaging of the rFLS–M1 macrophage co–culture model further confirmed early cell–cell interactions on day 1, followed by the appearance of elongated spindled-shaped rFLS and clustered macrophages by day 3 (Fig. 13A). This phenomenon were not observed in the rFLS– M0 macrophage co–culture model. Scanning electron microscopy and optical micrographs revealed that rFLS co-cultured with M1 macrophages developed an aggressive phenotype, characterized by increased spindle–shaped extensions and clustering of M1 macrophages (Fig. 13B & C). These features were absent in rFLS co-cultured with non-stimulated (M0) macrophages. In RA patients, the clustering of inflammatory macrophages within the synovial lining has been reported, and the clusters are often associated with various cell populations at different stages of disease progression[3,41].

Time–lapse videos of the rFLS–M0 and rFLS–M1 macrophage co-culture models further support these observations, showing specific interactions in the rFLS–M1 macrophage co–culture as early as day 1 (Supplementary Videos 3 & 4). The videos capture the cross-talk between cells, indicated by the transfer of the red tracker dye from M1 macrophage to non-labelled rFLS cells. This interaction confirms active cellular communication, which initially induced a morphological transition of rFLS from a spindle shape to a rounded form, followed by a reversion to an elongated spindle shape by day 3 (Fig. 13C). These morphological changes confirm successful cell-cell interactions. Overall, this *in vitro* RA model, incorporating both rFLS and

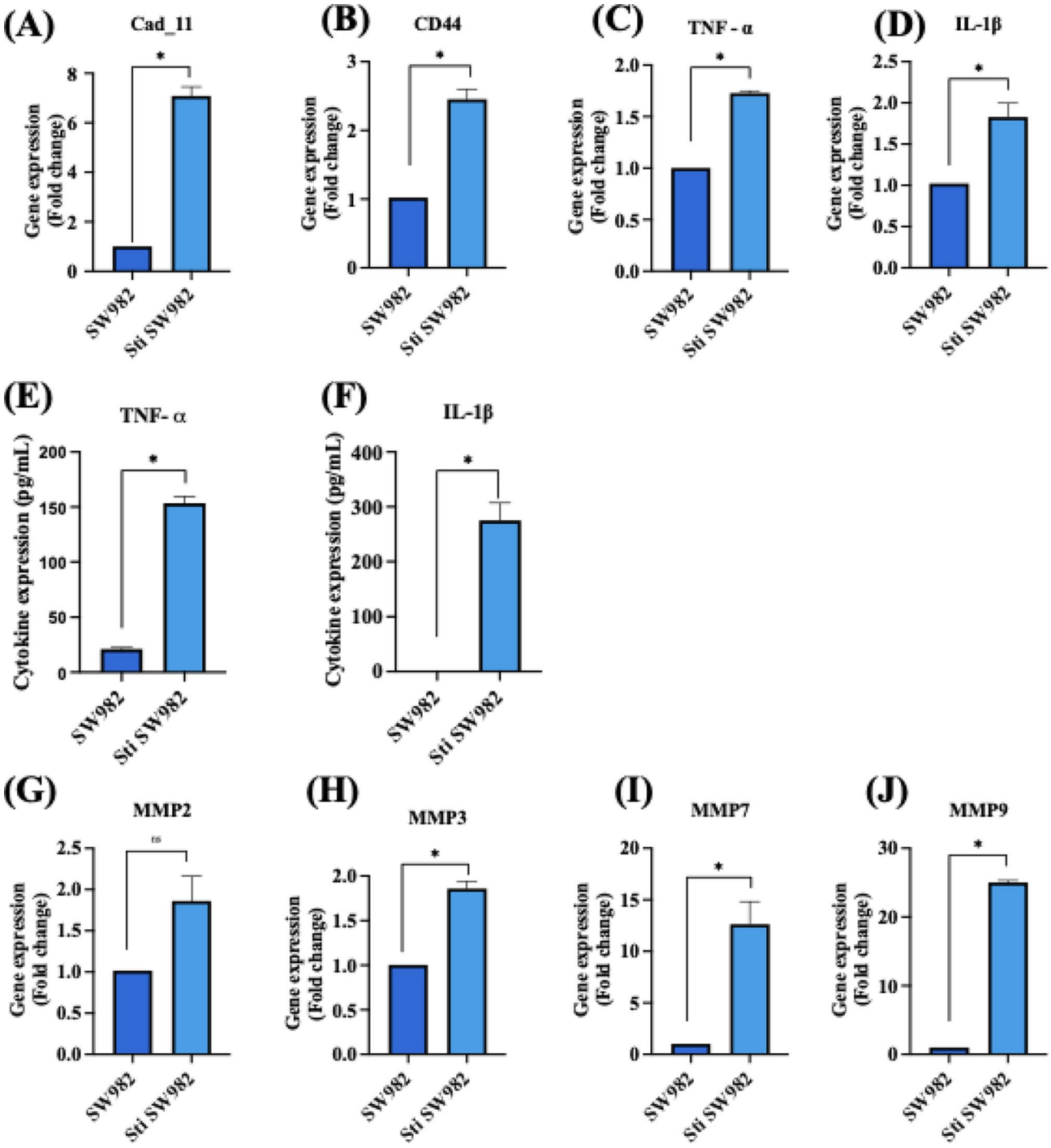

Fig. 9. Gene and protein expression analysis of non–stimulated and stimulated SW982 cells. qRT–PCR analysis of (**A**) cadherin–11, (**B**) CD44, (**C**) TNF–α, (**D**) IL–1β. ELISA quantification of inflammatory cytokine secretion levels of (**E**) TNF–α and (**F**) IL–1β. qRT–PCR analysis of matrix metalloproteinases (**G**) MMP2, (**H**) MMP3, (**I**) MMP 7 and (**J**) MMP 9. ($n = 3$; Student's t–test, $^{*}p < 0.05$).

macrophages, closely resembles the oxidative and inflammatory microenvironment characteristic of RA joints. It offers a robust platform for studying RA pathogenesis, including signaling pathways and cellular mechanisms.

Invasion potential of RA co-cultured in vitro model

Transwell and Matrigel® invasion assays demonstrated a significantly higher invasive capacity in the rFLS–M1 co–culture model compared to the rFLS–M0 model ($p < 0.05$), likely driven by the inflammatory and oxidative stress induced by M1 macrophages. This finding is consistent with *in vivo* characteristics of RA Synoviocytes, where elevated ROS levels and pro–inflammatory cytokines contribute to synovial hyperplasia and cartilage

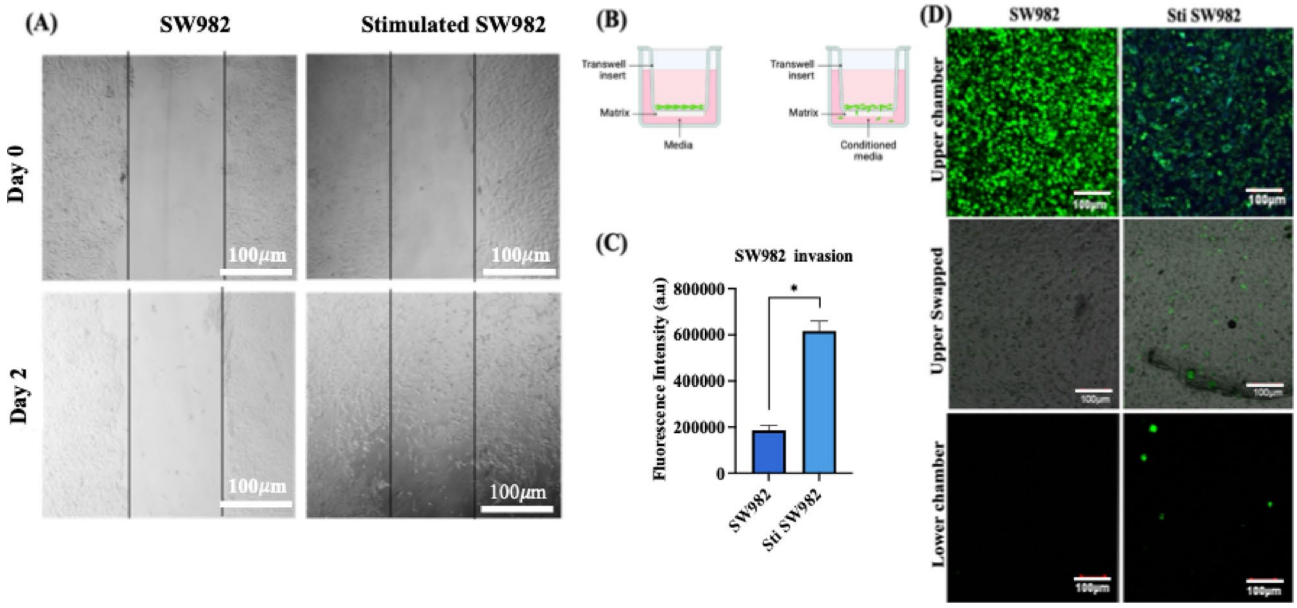

Fig. 10. (**A**) Wound closure assay illustrating the migration potential of stimulated Vs non–stimulated SW982 cells. (Scale bar: 100 μm); (**B**) Schematic representation of the Transwell invasion assay setup; (**C**) Quantification of fluorescence intensity of green-labelled SW982 cells that invaded the Matrigel® matrix toward chemoattractant in the lower chamber and (**D**) Representative CLSM images showing invasive SW982 cells under stimulated and non-stimulated conditions. (Scale bar: 100 μm) ($n = 3$; Student's t–test, $^*p < 0.05$).

invasion[31,33]. For the assay, red–labelled resting (M0) or activated (M1) macrophages were seeded in the lower chamber, while green-labelled rFLS were seeded onto Matrigel®–coated Transwell inserts and cultured for 24 h. Figure 14A & B illustrate the coexistence of green–labelled rFLS and red–labelled M1 macrophages in the lower chamber, confirming that rFLS successfully invaded through the Matrigel® matrix (Fig. 14B iii). In contrast, no green–labelled rFLS were detected in the lower chamber when it contained resting M0 macrophage (Fig. 14B ii), highlighting the role of activated M1 macrophages in promoting rFLS invasion.

In further experiments, green–labelled rFLS or SW982 cells were co-cultured with or without M1 macrophages, to validate these findings (Fig. 15 Ai & ii). The presence of rFLS in both the upper (after swapping) and lower chambers in the presence of M1 macrophages further demonstrated the ability of inflammatory M1 macrophages to promote rFLS invasiveness. The invasion of synovial fibroblast–like cells was significantly higher ($p < 0.05$) in the presence of M1 macrophages compared to non–stimulated controls (Fig. 15 Bi & ii). These results suggest that inflammatory cytokine secreted by M1 macrophages (discussed elsewhere) activate synovial fibroblast–like cells (rFLS and SW982), leading to the expression of key cell–cell interaction motifs, including CD44, Cad–11 and MMPs as reported in other sections of this study. These factors collectively contribute to the enhanced invasive behavior of activated FLS toward M1 macrophages.

Testing MTX as model drug on co-culture system

This simplified 2D co-culture system effectively mimics key characteristics of native RA, including the presence of both fibroblast-like synoviocytes (FLS) and macrophages representative of the intimal synovial layer, cell-cell interaction, expression of inflammatory cytokines and markers. Therefore, it provides a relevant platform for evaluating the therapeutic efficacy of various drug candidates. Testing compounds such as small molecules therapeutics, nanomedicines, or biologics, etc., in such a combinatorial cellular environment may yield more representative and clinically translatable data compared to conventional single-cell type assays. Methotrexate, a first-line anti-inflammatory drug commonly used for RA treatment, was tested in this co-culture system. Figure 16A - D illustrate the effects of MTX on cell stimulation and invasion in the presence of inflammatory macrophages. MTX significantly reduced invasion of both SW982 cells and rFLS through the ECM-mimicking Matrigel® matrix toward M1 macrophages, as compared to untreated controls. These findings highlight the potential of the rFLS–M1 or SW982-M1 co–culture model as a robust *in vitro* system for evaluating therapeutic efficacy, optimizing drug delivery strategies, and investigating the effects of therapeutics under inflammatory and hypoxic conditions that closely resemble the RA microenvironment.

Conclusion and future perspective

This study presents a simplified yet robust 2D co-culture model that mimics the inflammatory microenvironment of rheumatoid arthritis (RA) by modulating the ratio between fibroblast-like synoviocytes (FLS) and polarized macrophages. The model captures key RA hallmarks, including elevated ROS levels, increased expression of pro-inflammatory cytokines (TNF-α, IL-1β, IL-6), morphological transformation of FLS, and enhanced migration

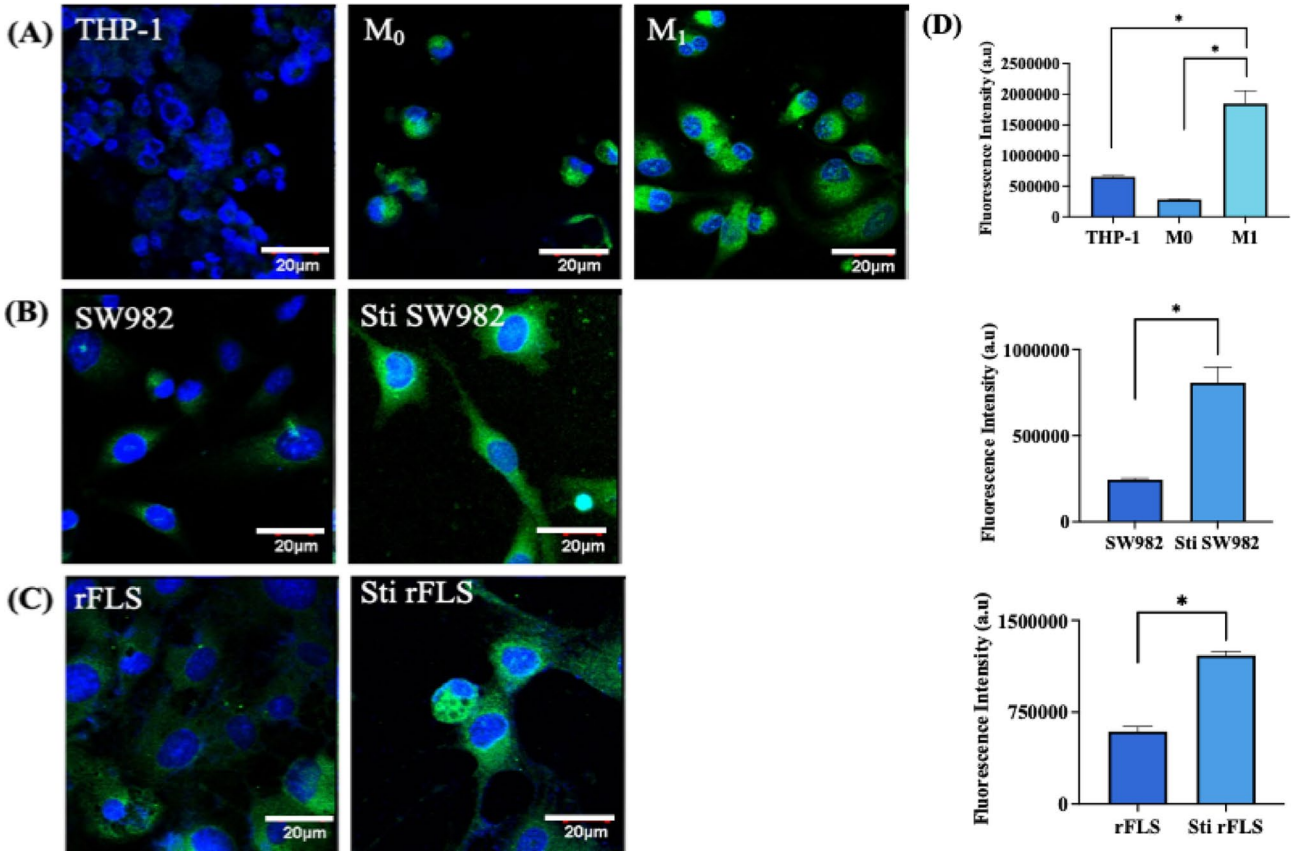

Fig. 11. Immunofluorescence analysis of hypoxia inducing factor–alpha (HIF-1α) expression in various cell types; (**A**) THP–1 monocytic cells, resting macrophage (M0) and activated macrophages (M1); (**B**) Human synovial sarcoma cell line SW982 and its stimulated counterpart; (**C**) Rat fibroblast–like–synoviocytes and stimulated rFLS. Cells were stained for HIF-1α (green) and counterstained with DAPI for nuclei (blue). Scale bar: 20 μm; (**D**) Quantification of HIF–1α fluorescence intensity across cell groups ($n = 3$). (Student's t–test & one-way ANOVA, $^*p < 0.05$).

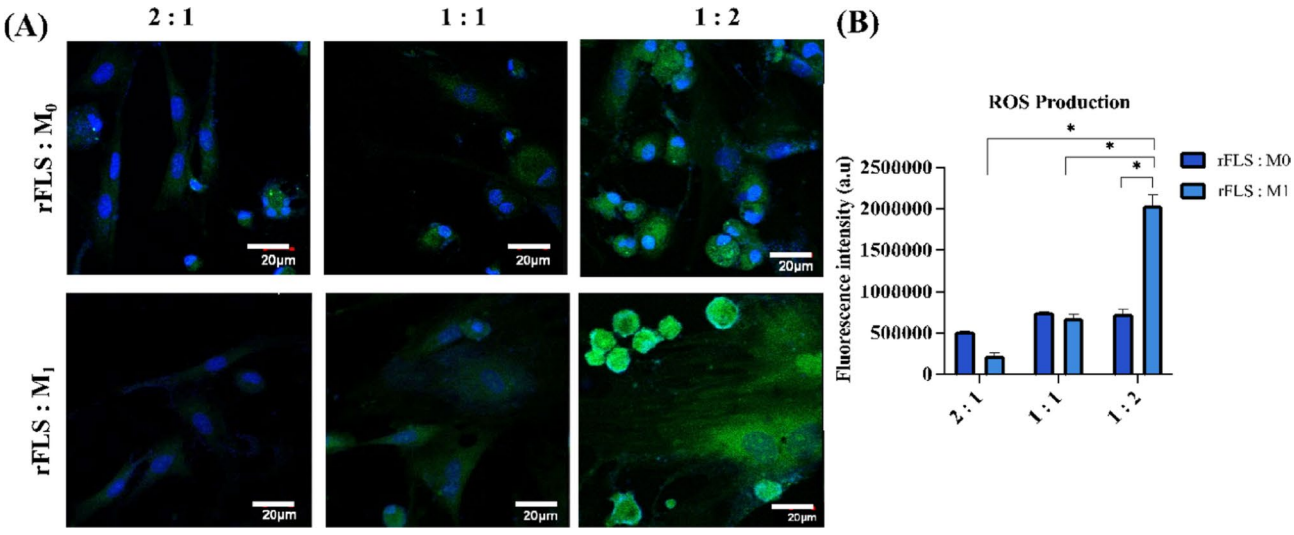

Fig. 12. Co-culture of synovial FLS and macrophage lineage cells; (**A**) CLSM images representing ROS production in FLS co-cultured with either M0 or M1 macrophages at varying ratios (FLS: macrophage = 2:1, 1:1 or 1:2) on day 3; ROS is visualized in green (DCFDA), and nuclei are counterstained with DAPI (blue). Scale bar = 20 μm. (**B**) Quantitative analysis of ROS fluorescence intensity from CLSM images ($n = 3$; Two-way ANOVA, $^*p < 0.05$).

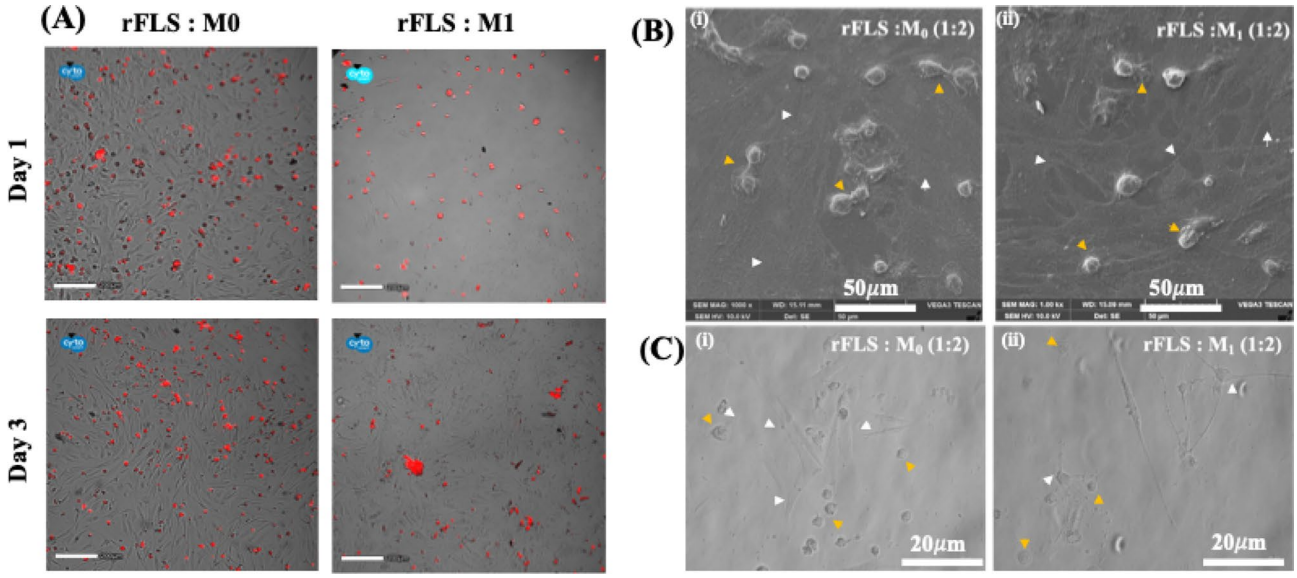

Fig. 13. (**A**) Fluorescence images representing the distribution of red-stained M0 or M1 macrophages co-cultured with rFLS at different time points (Scale bar: 200 μm); (**B**, **C**) SEM and optical micrographs representing the co-culture of FLS with either resting (M0) or inflammatory (M1) macrophages (yellow arrowheads: M0 or M1 macrophages; white arrowheads: rFLS cells). Scale bars: 20 μm (optical) and 50 μm (SEM).

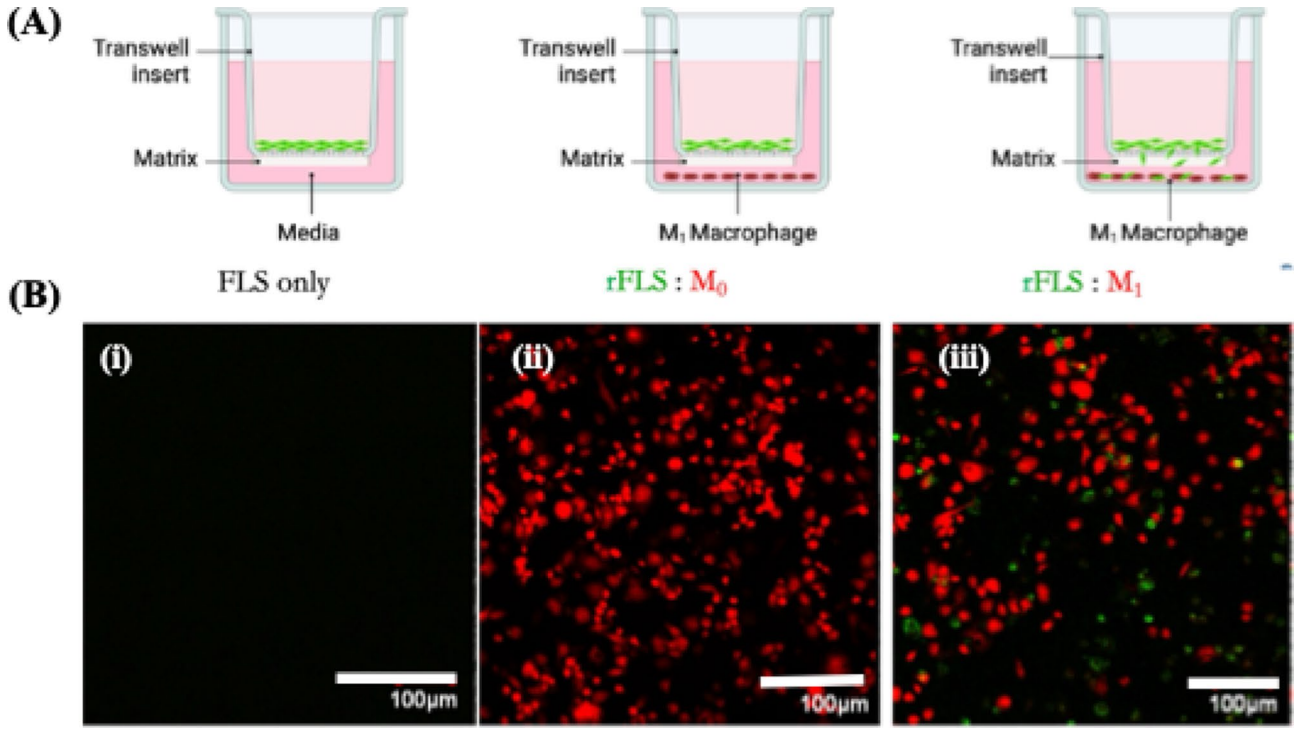

Fig. 14. Invasion assay of rFLS in the RA co-culture model (**A**) Schematic representation of the Trans–well co-culture setup; (**B**) Confocal laser scanning microscopy images showing invasion of green-labelled rFLS toward red-labelled inflammatory (M1) macrophages (Scale bar 100 μm).

and invasion driven by upregulated MMPs. Observable behaviors such as cell clustering and dynamic interactions between FLS and M1 macrophages reflect disease progression and offer insights into synovial cell crosstalk.

Compared to complex 3D systems, this 2D model offers a reproducible, scalable, and high-throughput-compatible platform without compromising physiological relevance. Its translational value is underscored by

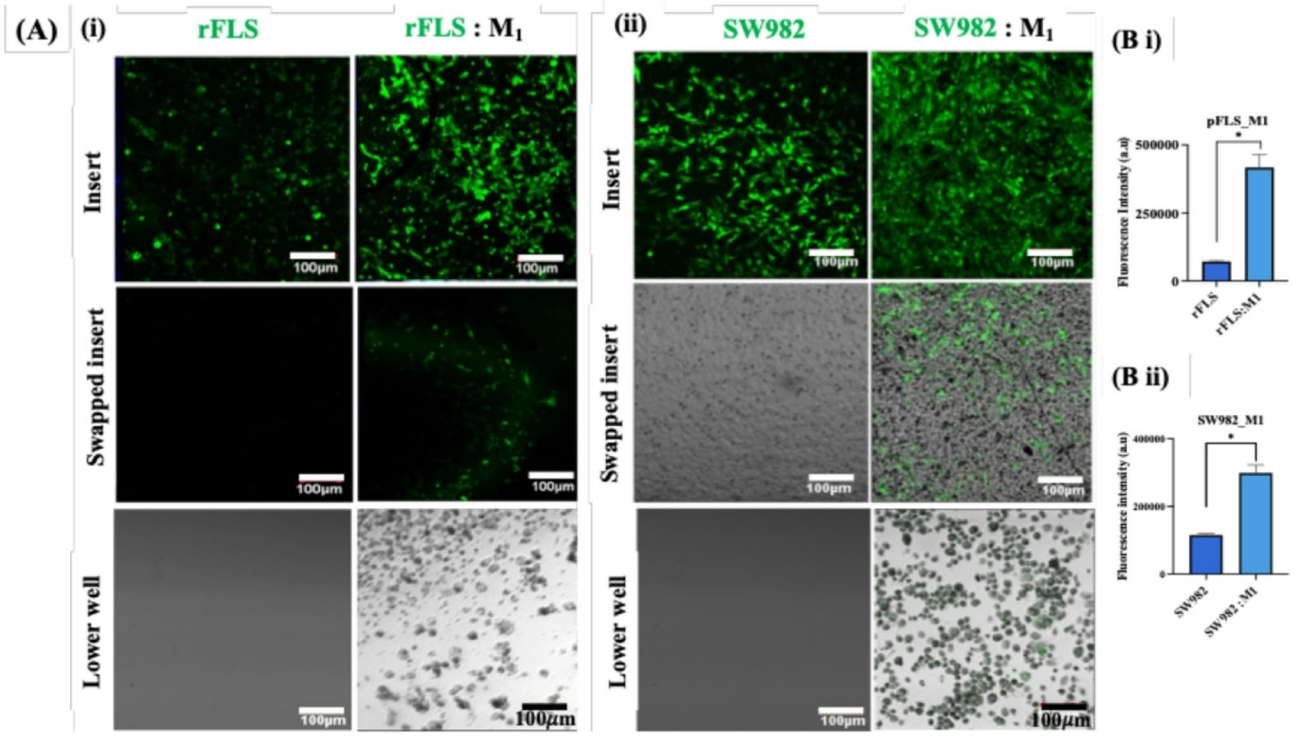

Fig. 15. Invasion of synovial fibroblast-like cells toward inflammatory macrophages. (**A**) CLSM images showing green-labelled primary rFLS and SW982 cells invading through the Matrigel® matrix towards M1 inflammatory macrophages in the lower chamber (Scale bar 100 μm); (**B**) Quantification of fluorescence intensity of invaded fibroblast-like cells within the Matrigel® matrix (i) Primary rFLS and (ii) SW982 cells co-cultured with M1 macrophages ($n = 3$; Student's t-test, $^{*}p < 0.05$).

Methotrexate's ability to reduce cell invasion in this setup, demonstrating its potential for evaluating therapeutic efficacy.

While this study center on macrophage–FLS interactions, immune cells like T and B lymphocytes are also crucial in RA pathogenesis. Future adaptations may incorporate these cell types using adherent or suspension cultures. Though this adds complexity, it can be addressed through advanced systems such as lab-on-chip or microfluidic platforms, enabling precise, physiologically relevant modelling of the RA synovial environment.

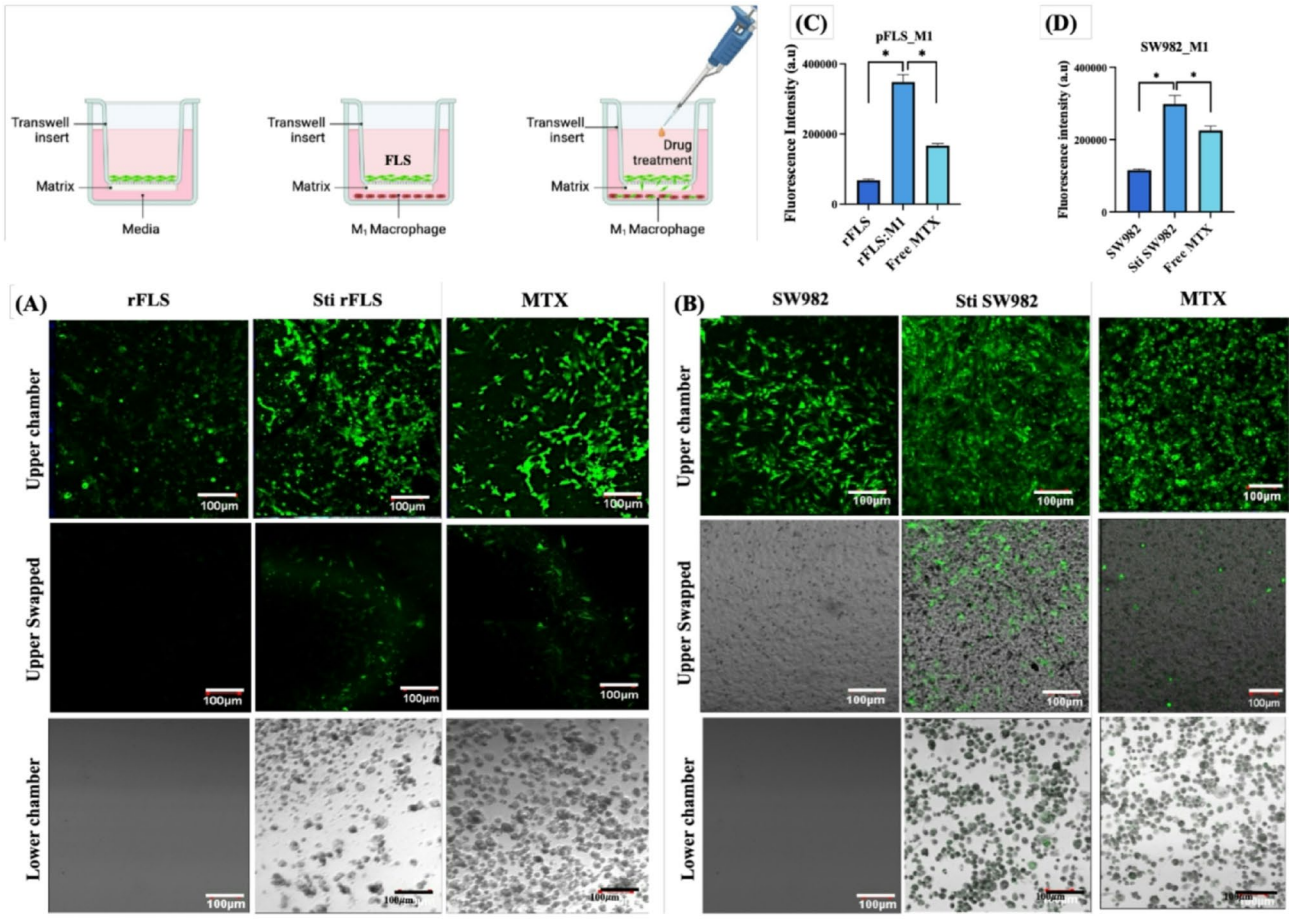

Fig. 16. Representative CLSM images showing the effect of Methotrexate (MTX) treatment on (**A**) rat primary fibroblast-like synoviocytes and (**B**) human SW982 cells co-cultured with M1 inflammatory macrophages; [C&D] Quantified fluorescence intensity of invaded cells through the Matrigel matrix ($n = 3$; One-way ANOVA, $^{*}p < 0.05$).

Data availability

All data generated or analysed during this study are included in this published article [and its supplementary information files].

Received: 1 February 2025; Accepted: 12 August 2025
Published online: 17 August 2025

References

1. Deshmukh, R. Rheumatoid arthritis: pathophysiology, current therapeutic strategies and recent advances in targeted drug delivery system. *Mater. Today Commun.* **35**, 105877 (2023).
2. Kai, K. et al. Synovial-tissue resident macrophages play Proinflammatory functions in the pathogenesis of RA while maintaining the phenotypes in the steady state. *Immunol. Med.* **47**, 58–67 (2024).
3. Kurowska-Stolarska, M. & Alivernini, S. Synovial tissue macrophages in joint homeostasis, rheumatoid arthritis and disease remission. *Nat. Rev. Rheumatol.* **18**, 384–397 (2022).
4. Müller-Ladner, U., Ospelt, C., Gay, S., Distler, O. & Pap, T. Cells of the synovium in rheumatoid arthritis. Synovial fibroblasts. *Arthritis Res. Ther.* **9**, 223 (2007).
5. Smith, D. The normal synovium. *Open. Rheumatol. J.* **5**, 100–106 (2011).
6. Zheng, Y. et al. Macrophage polarization in rheumatoid arthritis: signaling pathways, metabolic reprogramming, and crosstalk with synovial fibroblasts. *Front Immunol* **15**, (2024).
7. Bustamante, M. F., Garcia-Carbonell, R., Whisenant, K. D. & Guma, M. Fibroblast-like synoviocyte metabolism in the pathogenesis of rheumatoid arthritis. *Arthritis Res. Ther.* **19**, 110 (2017).
8. Yoo, S. A. et al. MIF allele-dependent regulation of the MIF coreceptor CD44 and role in rheumatoid arthritis. *Proc. Natl. Acad. Sci.* 113, E7917–E7926 (2016).
9. Kiener, H. P., Lee, D. M., Agarwal, S. K. & Brenner, M. B. Cadherin-11 induces rheumatoid arthritis Fibroblast-Like synoviocytes to form lining layers in vitro. *Am. J. Pathol.* **168**, 1486–1499 (2006).
10. Jonsson, A. H. Synovial tissue insights into heterogeneity of rheumatoid arthritis. *Curr. Rheumatol. Rep.* **26**, 81–88 (2024).
11. Choy, E. Understanding the dynamics: pathways involved in the pathogenesis of rheumatoid arthritis. *Rheumatology* **51**, v3–v11 (2012).

12. Thangadurai, M., Sethuraman, S. & Subramanian, A. Drug delivery approaches for rheumatoid arthritis: recent advances and clinical translation aspects. *Crit. Rev. Ther. Drug Carrier Syst.* **42**, 1–54 (2025).
13. Mousavi, M. J. et al. Transformation of fibroblast-like synoviocytes in rheumatoid arthritis; from a friend to foe. *Autoimmun. Highlights*. **12**, 3 (2021).
14. Kim, D. et al. 3D in vitro synovial hyperplasia model on polycaprolactone-micropatterned nanofibrous microwells for screening disease-modifying anti-rheumatic drugs. *Mater. Today Bio*. **26**, 101061 (2024).
15. Kannan, K., Ortmann, R. A. & Kimpel, D. Animal models of rheumatoid arthritis and their relevance to human disease. *Pathophysiology* **12**, 167–181 (2005).
16. Zhao, T. et al. How to model rheumatoid arthritis in animals: from rodents to Non-Human primates. *Front Immunol* **13**, (2022).
17. Guo, Q. et al. Rheumatoid arthritis: pathological mechanisms and modern Pharmacologic therapies. *Bone Res* **6**, (2018).
18. Wang, S. et al. Advances in experimental models of rheumatoid arthritis. *Eur. J. Immunol.* **53**, 2249962 (2023).
19. Sert, N. P. et al. The ARRIVE guidelines 2.0: updated guidelines for reporting animal research. *PLOS Biol.* **18**, e3000410 (2020).
20. Deng, X. et al. Effects of lycium barbarum polysaccharides with different molecular weights on function of RAW264.7 macrophages. *Food Agric. Immunol.* **29**, 808–820 (2018).
21. Takada, R. et al. Granulocyte macrophage colony-stimulating factor-induced macrophages of individuals with autism spectrum disorder adversely affect neuronal dendrites through the secretion of pro-inflammatory cytokines. *Mol. Autism*. **15**, 10 (2024).
22. Cheng, L. et al. Exosomes from melatonin treated hepatocellularcarcinoma cells alter the immunosupression status through STAT3 pathway in macrophages. *Int. J. Biol. Sci.* **13**, 723–734 (2017).
23. Heinrich, F. et al. Morphologic, phenotypic, and transcriptomic characterization of classically and alternatively activated canine blood-derived macrophages in vitro. *PLoS ONE*. **12**, e0183572 (2017).
24. Bian, Y. et al. Immunomodulatory roles of metalloproteinases in rheumatoid arthritis. *Front Pharmacol* **14**, (2023).
25. Dou, C., Yan, Y. & Dong, S. Role of cadherin-11 in synovial joint formation and rheumatoid arthritis pathology. *Mod. Rheumatol.* **23**, 1037–1044 (2013).
26. Row, S., Liu, Y., Alimperti, S., Agarwal, S. K. & Andreadis, S. T. Cadherin-11 is a novel regulator of extracellular matrix synthesis and tissue mechanics. *J. Cell. Sci.* **129**, 2950–2961 (2016).
27. Pulik, Ł., Łęgosz, P. & Motyl, G. Matrix metalloproteinases in rheumatoid Arthritis and osteoarthritis: a state of the Art review. *Reumatologia* **61**, 191–201 (2023).
28. Więcek, K., Kupczyk, P., Chodaczek, G. & Woźniak, M. The Impact of Curcumin on the Inflammatory Profile of SW982 Cells in a Rheumatoid Arthritis Model. *J. Immunol. Res.* e1208970 (2022). (2022).
29. Chang, J. H., Lee, K. J., Kim, S. K., Yoo, D. H. & Kang, T. Y. Validity of SW982 synovial cell line for studying the drugs against rheumatoid arthritis in fluvastatin-induced apoptosis signaling model. *Indian J. Med. Res.* **139**, 117–124 (2014).
30. Tsuneki, M. & Madri, J. A. CD44 influences fibroblast behaviors via modulation of Cell-Cell and Cell-Matrix interactions, affecting survivin and Hippo pathways: CD44 MODULATES FIBROBLAST CELL ADHESION. *J. Cell. Physiol.* **231**, 731–743 (2016).
31. Naor, D. & Nedvetzki, S. CD44 in rheumatoid arthritis. *Arthritis Res. Ther.* **5**, 105–115 (2003).
32. Chang, S. K., Gu, Z. & Brenner, M. B. Fibroblast-like synoviocytes in inflammatory arthritis pathology: the emerging role of cadherin-11. *Immunol. Rev.* **233**, 256–266 (2010).
33. Valencia, X. et al. Cadherin-11 provides specific cellular adhesion between fibroblast-like synoviocytes. *J. Exp. Med.* **200**, 1673–1679 (2004).
34. Ding, Q. et al. Signaling pathways in rheumatoid arthritis: implications for targeted therapy. *Signal. Transduct. Target. Ther.* **8**, 1–24 (2023).
35. Lefèvre, S. et al. Synovial fibroblasts spread rheumatoid arthritis to unaffected joints. *Nat. Med.* **15**, 1414–1420 (2009).
36. Neumann, E. et al. Migratory potential of rheumatoid arthritis synovial fibroblasts: additional perspectives. *Cell. Cycle*. **9**, 2286–2291 (2010).
37. Qiu, B. et al. Hypoxia inducible factor-1α is an important regulator of macrophage biology. *Heliyon* **9**, e17167 (2023).
38. Hu, F. et al. Hypoxia-inducible factor-1α perpetuates synovial fibroblast interactions with T cells and B cells in rheumatoid arthritis. *Eur. J. Immunol.* **46**, 742–751 (2016).
39. Li, H. et al. The pathogenesis and regulatory role of HIF-1 in rheumatoid arthritis. *Cent. -Eur J. Immunol.* **48**, 338–345 (2023).
40. Jing, W. et al. Role of reactive oxygen species and mitochondrial damage in rheumatoid arthritis and targeted drugs. *Front Immunol* **14**, (2023).
41. Alivernini, S. et al. Distinct synovial tissue macrophage subsets regulate inflammation and remission in rheumatoid arthritis. *Nat. Med.* **26**, 1295–1306 (2020).

Acknowledgements

Few schematic images are created with Biorender.com.

Author contributions

Anuradha Subramanian and Madhumithra Thangadurai designed this study. Madhumithra Thangadurai have performed the experiments, analyzed data and drafted the manuscript. Anuradha Subramanian verified the data. Anuradha Subramanian and Swaminathan Sethuraman critically revised the manuscript. All authors have read and approved the final manuscript.

Funding

Authors sincerely thank SASTRA Deemed University for providing T.R.R. Research fund (No. SASTRA–TRR–1–13122023) and Department of Biotechnology (BT/PR26760/NNT/28/1433/2017), Nano Mission (SR/NM/NS–1205/2015(G)) Department of Science and Technology, Government of India for the financial support.

Declarations

Competing interests

The authors declare no competing interests.

Ethics approval

Ethical approval has been obtained from Institutional Animal Ethical Committee approval (IAEC Approval number: 666/SASTRA/IAEC/RPP) to obtain synovial tissues from Rat knee joints. The procedure followed in this study are in compliance with ARRIVE guidelines.

Additional information

Supplementary Information The online version contains supplementary material available at https://doi.org/10.1038/s41598-025-16007-3.

Correspondence and requests for materials should be addressed to A.S.

Reprints and permissions information is available at www.nature.com/reprints.

Publisher's note Springer Nature remains neutral with regard to jurisdictional claims in published maps and institutional affiliations.